Click Here for Full Article

Distribution of recycled crust within the upper mantle: Insights from the oxygen isotope composition of MORB from the Australian-Antarctic Discordance

Kari M. Cooper
Geology Department, University of California, One Shields Avenue, Davis, California 95616, USA (kmcooper@ucdavis.edu)

John M. Eiler
Division of Geological and Planetary Sciences, Caltech, Pasadena, California 91125, USA

Kenneth W. W. Sims
Department of Geology and Geophysics, Woods Hole Oceanographic Institution, Woods Hole, Massachusetts 02543, USA

Now at Department of Geology and Geophysics, University of Wyoming, Laramie, Wyoming 82071, USA

Charles H. Langmuir
Department of Earth and Planetary Sciences, Harvard University, Cambridge, Massachusetts 02138, USA

[1] Geochemical heterogeneity within the mantle has long been recognized through the diversity of trace element and radiogenic isotopic compositions of mantle-derived rocks, yet the specific origin, abundance, and distribution of enriched material within the mantle have been difficult to quantify. In particular, the origin of the distinctive geochemical characteristics of Indian mantle has been debated for decades. We present new laser fluorination oxygen isotope measurements of mid-ocean ridge basalt from the Australian-Antarctic Discordance (AAD), an area where a particularly abrupt transition occurs between Pacific-type mid-ocean ridge basalts (MORB) and Atlantic-type MORB. These data show no distinction in average $\delta^{18}O$ between Pacific- and Atlantic-type MORB, indicating that the origin of Indian-type mantle cannot be attributed to the presence of pelagic sediment. The combined radiogenic isotope, $\delta^{18}O$, and trace element characteristics of Indian-type MORB at the AAD are consistent with contamination of the Indian upper mantle by lower crustal material. We also present a compilation of available laser fluorination $\delta^{18}O$ data for MORB and use these data to evaluate the nature and percentage of enriched material within the upper mantle globally. Data for each ocean basin fit a normal distribution, with indistinguishable means and standard deviations, implying that the variation in $\delta^{18}O$ of MORB reflects a stochastic process that operates similarly across all ocean basins. Monte Carlo simulations show that the mean and standard deviation of the MORB data are robust indicators of the mean and standard deviation of the parent distribution of data. Further, although some skewness in the data cannot be ruled out, Monte Carlo results are most consistent with a normal parent distribution. This similarity in characteristics of the $\delta^{18}O$ data between ocean basins, together with correlations of $\delta^{18}O$ with radiogenic isotope and trace element characteristics of subsets of the data, suggest that the upper mantle globally contains an average of ~5–10% recycled crustal material and that the depleted mantle in the absence of this component would have $\delta^{18}O$ of ~5.25‰. The Monte Carlo simulations also suggest that additional oxygen isotope data may be used in the future to test the ability of geodynamical models to predict the physical distribution of enriched domains within the upper mantle.

1. Introduction

[2] The origin and physical distribution of domains of different composition within the mantle has been the subject of study for decades. Diverse, complementary approaches have been taken to this problem, including studies of the variations in geochemical characteristics of oceanic basalts [e.g., *Hofmann*, 2003, and references therein] and numerical simulations of mixing and stirring of recycled crust as a consequence of mantle circulation [e.g., *Brandenburg et al.*, 2008; *Christensen and Hofmann*, 1994; *Kellogg et al.*, 1999; *Tackley*, 2000; *van Keken et al.*, 2002; *Xie and Tackley*, 2004]. Geochemical variations in oceanic basalts have long been attributed in part to the presence of recycled crustal material [e.g., *Zindler and Hart*, 1986], and, although the greatest range in composition is seen in oceanic island basalts (OIB), there is substantial heterogeneity within the upper mantle sampled by mid-ocean ridge basalts (MORB) as well [e.g., *Cohen et al.*, 1980; *Dupre and Allegre*, 1983; *Hart*, 1971, 1984; *Hofmann*, 2003, and references therein; *Salters and Stracke*, 2004; *Schilling et al.*, 1983; *Tatsumoto et al.*, 1965; *Workman and Hart*, 2005]. This heterogeneity is manifest as a range in radiogenic isotope composition (e.g., Pb, Nd, Sr, Hf) in MORB globally, even in areas of ridge axis not obviously influenced by hot spots. In addition to the heterogeneity present within MORB from any given ocean basin, MORB compositions appear to be systematically different between different ocean basins. In particular, the Indian ocean basin has distinctive Pb-Nd-Sr-Hf isotope compositions compared to Pacific or Atlantic MORB, and the origin of these distinctions has been attributed to the addition of local "plume" material [*Pyle et al.*, 1995], recycled pelagic sediment [*Rehkämper and Hofmann*, 1997], subduction-modified mantle wedge material [*Gurnis et al.*, 1998; *Kempton et al.*, 2002], or

recycled continental lithospheric mantle or lower crust [*Hanan et al.*, 2004; *Janney et al.*, 2005].

[3] The geochemical heterogeneity present in MORB reflects the size, spatial distribution, and nature (origin and age) of domains within the upper mantle that are enriched or depleted in incompatible elements relative to bulk Earth (following convention, we refer to these as "enriched" and "depleted" mantle, respectively). This heterogeneity is averaged to some extent by the process of MORB melt generation, which samples a finite volume of the upper mantle, and which may preferentially sample enriched domains due to their higher melt productivity relative to depleted mantle. A number of workers have modeled the geochemical effects of sampling this heterogeneity [e.g., *Albarede*, 2001; *Allegre et al.*, 1987; *Kellogg et al.*, 2002, 2007; *Meibom and Anderson*, 2004; *Prinzhofer et al.*, 1989; *Rudge et al.*, 2005]; for example, *Kellogg et al.* [2002, 2007] examined the combined effects of sizes of enriched domains and the sampling (i.e., melting) process on the Sr-Nd-Pb isotopic systems and found that the range of isotopic compositions produced was dependent on the length scale of sampling relative to the length scale of the heterogeneities. However, interpretations of these and other trace element and radiogenic isotope data are complicated by the effects of aging on radiogenic isotope ratios and by strong contrasts in trace element concentration between enriched and depleted mantle and between different potential types of enriched mantle. Both ^{18}O and ^{16}O are stable, nonradiogenic isotopes; therefore, oxygen isotope compositions of rocks are unaffected by radioactive decay, allowing investigation of the nature of the enriched material without the complicating effects of the tradeoff in radiogenic isotope studies between differences in parent-daughter ratios and duration of radiogenic ingrowth. Furthermore, oxygen isotopic composi-

tions of rocks are relatively weakly influenced by high-temperature mantle processes (e.g., melting), but are strongly fractionated during interactions of rocks and the hydrosphere near the Earth's surface. Therefore, measurement of oxygen isotope compositions of MORB offers an opportunity to examine the geochemical effects of enriched crustal material present within the upper mantle without complicating effects of age or large variations in concentration.

[4] The Australian-Antarctic Discordance (AAD) is one of the deepest sections of mid-ocean ridge, reflecting a relatively cold mantle and slow spreading rates [Klein et al., 1991; Pyle et al., 1992, 1995]. In addition, there is an exceptionally sharp boundary between Pacific-type MORB erupted in the eastern sections of the AAD and Indian-type MORB erupted to the west, occurring over <25 km of the ridge axis [Kempton et al., 2002; Pyle et al., 1992, 1995]. Thus, samples of MORB from the AAD provide an opportunity to examine the origin of Indian upper mantle compared to Pacific upper mantle, without the complicating effects of variations in spreading rate or melting parameters. We present new oxygen isotope data for samples of Indian-type and Pacific-type MORB from the AAD, and use these data to evaluate models of formation of the Indian-type mantle. We also present a compilation of currently available high-precision laser fluorination $\delta^{18}O$ data for MORB globally, and examine the characteristics of the distribution of data between ocean basins in order to better understand the implications of the data for the nature, physical distribution and percentage of crustal material in the upper mantle.

2. Samples and Methods

[5] Samples were collected by dredging during cruises in 1975 and 1976 by the R/V Vema and in 1988 during cruise MW8801 of the R/V Moana Wave, and the samples used here have been studied previously for major and trace element compositions and radiogenic isotopic compositions [Hanan et al., 2004; Kempton et al., 2002; Klein et al., 1988, 1991; Pyle et al., 1992, 1995] (Table 1). Splits of each of 16 samples were crushed by hand and fresh, phenocryst-free glass separates were prepared by hand picking under a binocular microscope. Aliquots of 1–2 mg each were analyzed by laser fluorination at the California Institute of Technology using a 50W CO_2 laser, BrF_5 reagent, and an apparatus for gas purification and conversion of O_2 to CO_2 based on designs by Sharp

[1990] and Valley et al. [1995]. Oxygen yields were 13.5 ± 1.0 μmol/mg, typical of yields for laser fluorination measurements of fresh glasses [e.g., Cooper et al., 2004; Eiler et al., 2000b]. Measurements of $\delta^{18}O$ were made on 4 separate days. On each day five to ten analyses of standards (including in-house glass standards AH95-22 [Eiler et al., 2000b] and ALV526-1 and garnet standard UWG-2 [Valley et al., 1995] were made; reproducibility for repeat measurements of each standard on a given day averaged 0.05‰ (1σ). The mean $\delta^{18}O$ values for standards were within ~0.18‰ of their nominal values based on previous analyses. All data on unknowns collected on a given day were corrected by a constant value equal to the average difference between measured and accepted values for standards measured on that day. Because the garnet standard has been used in a number of previous studies and its composition is best known, and to assure consistency with the data collected on other MORB glasses in the same lab, we corrected the unknown analyses based on the nominal value of 5.75‰ for UWG-2. Unknown samples were analyzed two to five times on the same day, with an average standard error of the mean for multiple analyses of the same sample of ±0.03‰ (1σ). None of the AAD samples in this study were analyzed on separate days; however, in similar studies from the same lab where aliquots of the same sample were analyzed on multiple days [e.g., Cooper et al., 2004; Eiler et al., 2000b] reproducibility of replicate analyses was similar to this study.

[6] We have compiled a data set of high-precision laser fluorination measurements of $\delta^{18}O$ in MORB (Table S1 in the auxiliary material).[1] All data compiled in Table S1 have been published previously, with the exception of oxygen isotope measurements of MORB from the 9–10°N region of the EPR. We analyzed $\delta^{18}O$ in a subset of the samples studied by Sims et al. [2002, 2003] at Caltech using the methods described above for the AAD samples. Oxygen yields were 12.2 ± 0.8 μmol/mg. Measurements of $\delta^{18}O$ were made on 6 separate days. On each day six to eleven analyses of standards (including garnet standard UWG-2 [Valley et al., 1995] and olivine standard SCO-3) were made; reproducibility for repeat measurements of each standard on a given day averaged 0.05‰ (1 standard deviation), 0.02‰ average standard error of the mean. The mean $\delta^{18}O$ values for standards were within 0.19‰ of their nominal values based on previous analyses on all but 1 day of analyses,

---
[1]Auxiliary materials are available in the HTML. doi:10.1029/2009GC002728.

and were offset 0.35‰ on the remaining day. Unknown samples were analyzed two to five times on the same day, with an average standard error of the mean for multiple analyses of the same sample of ±0.03‰ (1σ). Five samples were analyzed on multiple days; the average standard error of the mean for those five samples was 0.06‰.

3. Results

[7] Oxygen isotope measurements for the AAD samples are presented in Figures 1 and 2 and, together with selected major element, trace element, and radiogenic isotopic data (from previously published studies), in Table 1. Other analyses of these samples have been published [*Hanan et al.*, 2004; *Kempton et al.*, 2002; *Klein et al.*, 1988, 1991; *Pyle et al.*, 1992, 1995] but are not reproduced here. The total range in δ^{18}O of the AAD samples is 0.37‰ (from 5.34‰ to 5.71‰), with an average of 5.46‰. The oxygen isotope composition of the AAD samples is compared to other laser fluorination measurements of MORB in Figure 2. The mean and range of our AAD data set are comparable to those of a global survey of NMORB (mean of 5.50‰, range of 0.44‰ [*Eiler et al.*, 2000b]), from the Mid-Atlantic Ridge (mean of 5.52‰ and range of 0.47‰ [*Cooper et al.*, 2004]), and from the 9–10°N region of the EPR (mean of 5.56‰, range of 0.33‰) (Table S1). There are no systematic differences in δ^{18}O between Indian (I-MORB) or Pacific (P-MORB) types within the AAD data (as distinguished by an established classification scheme based on radiogenic isotope data [*Kempton et al.*, 2002; *Pyle et al.*, 1992]); mean values of δ^{18}O are 5.48‰ and 5.41‰ for AAD I-MORB and P-MORB, respectively, indistinguishable within 95% confidence (as measured by the two times the standard error of the mean, 2SE = 0.076‰ for I-MORB and 0.07‰ for I-MORB (Figure 1)). As with other isotopic tracers [e.g., *Pyle et al.*, 1992], δ^{18}O in I-MORB AAD appears to be more heterogeneous than in the AAD P-MORB, as measured by the standard deviation of the I-MORB data (0.12) compared to that of the P-MORB data (0.09).

4. Discussion

4.1. Oxygen Isotopes in AAD MORB: Origin of the Indian MORB Source

[8] Indian MORB are distinguished from Atlantic and Pacific type MORB by having lower ^{206}Pb/^{204}Pb for a given ^{207}Pb/^{204}Pb and ^{208}Pb/^{204}Pb, relatively radiogenic (i.e., higher) ^{87}Sr/^{86}Sr and relatively unradiogenic (i.e., lower) ^{143}Nd/^{144}Nd [e.g., *Dupre and Allegre*, 1983; *Hart*, 1984]. A distinction in Pb-Nd-Hf isotope compositions has also been noted between Indian and Pacific MORB across the AAD, with I-MORB samples having higher Δ^{208}Pb (deviation of ^{208}Pb/^{206}Pb from the Northern Hemisphere reference line, as defined by *Hart* [1984]), associated with higher ε_{Hf} and lower ε_{Nd}, than P-MORB samples [*Hanan et al.*, 2004; *Kempton et al.*, 2002]. The chemical distinction between Indian and Pacific MORB has been attributed to the addition of enriched material to the upper mantle in the form of (1) an enriched mantle component related to the Kerguelen mantle plume and dispersed throughout the Indian upper mantle during rifting of Australia and Antarctica [e.g., *Pyle et al.*, 1995]; (2) recycled pelagic sediment [e.g., *Rehkämper and Hofmann*, 1997]; (3) subduction-modified mantle wedge material [*Gurnis and Muller*, 2003; *Gurnis et al.*, 1998; *Kempton et al.*, 2002]; or (4) recycled continental lithosphere, either as lithospheric mantle [e.g., *Hawkesworth et al.*, 1986; *Janney et al.*, 2005; *Mahoney et al.*, 1991] or as lower crust [*Escrig et al.*, 2004; *Hanan et al.*, 2004; *Janney et al.*, 2005]. In order to account fully for the isotopic distinctions between Indian and Pacific MORB, at least three components are required [e.g., *Rehkämper and Hofmann*, 1997], allowing for the possibility that more than one of the above components may play a role.

[9] As discussed above, the Australian-Antarctic Discordance (AAD) is of great interest in studying the origin of geochemical distinctions between the MORB source in different oceanic basins because a sharp geochemical boundary between Pacific and Indian type MORB allows investigation of the isotopic and trace element characteristics of Indian versus Pacific MORB sources without the complicating factors of differences in spreading rate, mantle temperature, degree of melting, or upwelling rate, [e.g., *Christie et al.*, 1998; *Gurnis and Muller*, 2003; *Hanan et al.*, 2004; *Kempton et al.*, 2002; *Klein et al.*, 1988; *Pyle et al.*, 1992, 1995]. Oxygen isotope data are particularly sensitive to the presence of materials that were once at the Earth's surface, and some of the types of enriched material described above should have distinctive oxygen isotopic compositions, allowing us to test some of the previous models for the origin of the distinctive chemistry of Indian MORB sources. In

Table 1. The $\delta^{18}O$, Major Element, Trace Element, and Radiogenic Isotope Data for AAD Samples Analyzed in This Study[a]

| Sample Name	D1-2	D2-19	D3-4	D4-1	D5-5	MOA8801-017-026	D7-3	D7-7	D8-8	D9-1	D11-6	D10-10	MOA8801-027-058	BMRG05-30-4	MOA8801-022-013	MOA8801-023-001
AAD zone	A3	A3	A3	A3	B5	A1	B3	B3	B1	C	C	C	B3	B4	B4	B4
Type	Pacific	Pacific	Pacific	Pacific	Pacific	Pacific	Indian	Indian	Indian	Indian	Indian	Indian	Indian	Indian	Indian	Indian
Latitude (°S)	50.41	50.27	50.42	50.22	48.74	50.222	49.03	49.03	49.47	49.81	49.86	49.92	49.062	49.41	49.68	49.613
Longitude (°E)	131.01	132.55	135.09	137.55	127.08	127.417	124	124	121.03	119.18	118	115.38	124.965	125.67	125.892	125.658
$\delta^{18}O$	5.38	5.55	5.43	5.34	5.42	5.31	5.45	5.55	5.36	5.51	5.38	5.71	5.64	5.37	5.49	5.40
Number of replicates	3	2	2	3	2	2	2	3	3	3	5	3	2	2	2	2
1σ	0.03	0.08	0.10	0.10	0.05	0.01	0.02	0.03	0.02	0.07	0.03	0.01	0.04	0.19	0.11	0.05
SiO_2	49	49.82	48.73	49.69	50.16	50.62	51.22	49.93	50.98	50.24	48.81	50.91	51.231	51.67	51.07	51.34
TiO_2	2.02	1.95	1.61	1.55	1.27	1.36	1.58	1	1.25	1.32	1.04	1.03	1.51	1.15	0.99	1.12
Al_2O_3	15.43	13.83	15.43	14.57	15.84	15.49	16.21	17.18	16.14	15.51	17.08	15.97	17.131	15.78	16.41	16.26
Fe_2O_3	10.77	12.6	10.27	11.23	9.42	8.44	9.14	8.07	8.39	9.54	8.96	8.67	7.967	9.37	7.75	9.18
MnO	0.18	0.21	0.17	0.12	0.16	0.15	0.16	0.14	0.15	0.16	0.15	0.15	0.171	0.20	0.13	0.13
MgO	8.69	7.01	8.03	8.05	8.66	8.37	7.33	9.11	7.94	8.34	9.22	8.72	7.17	7.36	8.33	7.71
CaO	10.39	11.13	11.69	12.1	11.5	11.54	10.06	11.23	10.97	11.66	11.28	11.47	10.198	11.62	10.97	10.86
Na_2O	2.95	2.84	2.9	2.64	2.92	2.93	3.72	2.99	3.26	2.73	3.02	2.88	3.71	2.87	3.19	2.87
K_2O	0.30	0.09	0.13	0.07	0.07	0.03	0.30	0.13	0.36	0.11	0.08	0.12	0.567	0.16	0.12	0.10
P_2O_5	0.29	0.18	0.18	0.13	0.13	0.15	0.23	0.12	0.17	0.13	0.11	0.12	0.23	0.11	0.17	0.15
Total	100.0	99.7	99.1	100.2	100.1	99.09	100.0	99.9	99.6	99.7	99.8	100.0	99.9	100.3	99.1	99.7
La	8.15	4.27	4.62	3.00	2.24	2.11	7.05	3.50	6.91	3.68	2.60	3.24	8.91	3.22	2.91	2.15
Ce	22.7	15.51	15.37	10.37	8.34	8.84	19.85	9.91	16.98	10.68	8.64	9.21	20.5	8.72	8.10	6.69
Pr	n.d.	n.d.	n.d.	n.d.	n.d.	1.61	n.d.	n.d.	n.d.	n.d.	n.d.	n.d.	2.96	1.46	1.38	1.12
Nd	16.52	13.49	11.92	9.64	8.14	9.36	14.3	8.07	10.79	9.19	7.64	7.66	12.8	7.28	7.18	6.24
Sm	4.74	4.65	3.7	3.52	2.72	3.31	4.29	2.71	3.29	3.2	2.6	2.6	3.71	2.55	2.38	2.33
Eu	1.71	1.66	1.42	1.33	1.07	1.27	1.49	1.06	1.21	1.21	1.04	0.97	1.34	1.01	0.90	0.92
Gd	5.69	6.23	4.53	4.8	3.73	4.23	5.31	3.62	3.95	4.19	3.38	3.53	4.75	3.59	3.08	3.03
Tb	n.d.	n.d.	n.d.	n.d.	n.d.	0.82	n.d.	n.d.	n.d.	n.d.	n.d.	n.d.	0.80	0.68	0.57	0.59
Dy	6.42	7.15	4.79	5.45	4.42	5.27	5.88	4.15	4.49	4.72	3.85	4.36	5.07	4.45	3.82	3.96
Ho	n.d.	n.d.	n.d.	n.d.	n.d.	1.11	n.d.	n.d.	n.d.	n.d.	n.d.	n.d.	1.10	0.98	0.83	0.87
Er	3.77	4.47	3.01	3.57	2.64	3.26	3.63	2.75	2.75	3	2.48	2.7	3.18	2.82	2.44	2.52
Tm	n.d.	n.d.	n.d.	n.d.	n.d.	0.51	n.d.	n.d.	n.d.	n.d.	n.d.	n.d.	0.50	0.45	0.40	0.40
Yb	3.63	4.34	2.8	3.24	2.55	3.13	3.46	2.31	2.46	2.86	2.23	2.46	3.05	2.76	2.37	2.47
Lu	0.578	0.65	0.419	0.513	0.3801	0.46	0.528	0.358	0.389	0.453	0.346	0.377	0.46	0.43	0.36	0.37
Ba	24.6	5.3	6	3.7	6.7	3.21	38.3	16.3	68.2	14.6	10.9	14.9	118.1	26.75	14.62	14.49
Co	n.d.	n.d.	n.d.	n.d.	n.d.	43.6	n.d.	n.d.	n.d.	n.d.	n.d.	n.d.	37.2	40.2	39.3	42.5
Cr	310	146	311	271	393	433	288	316	300	349	337	375	248.3	317	323	343
Cs	n.d.	n.d.	n.d.	n.d.	n.d.	0.015	n.d.	n.d.	n.d.	n.d.	n.d.	n.d.	0.18	0.054	0.015	0.019
Cu	53	68	76	72	72	75	53	61	86	61	72	63	51.7	73	72	83
Ni	157	57	100	76	131	104	96	155	116	114	166	119	110.2	115	145	149
Sc	35.8	42.5	39.3	41.2	35.2	37.1	30	28.2	32.2	35.8	30.1	33.2	30.5	38.8	33.7	35.0
Sr	240	115	178	110	132	n.d.	179	152	177	123	146	142	n.d.	n.d.	n.d.	n.d.
V	291	354	273	315	255	272	232	183	218	254	198	219	202.0	212	206	196
Y	39	41.5	32.9	34.4	28.7	28.7	34.3	24.4	26.2	29.1	25	25.4	31.8	28.0	25.0	24.5

Table 1. (continued)

Sample Name	D1-2	D2-19	D3-4	D4-1	D5-5	MOA8801-017-026	D7-3	D7-7	D8-8	D9-1	D11-6	D10-10	MOA8801-027-058	BMRG05-30-4	MOA8801-022-013	MOA8801-023-001
Zr	198	138	138	104	95	88	152	82	103	95	82	83	129.1	75	72	65
Nd MS-ID	16.01	13.15	12.2	9.44	8.58	n.d.	14.48	7.66	10.76	9.06	7.49	7.72	n.d.	n.d.	n.d.	n.d.
Sm MS-ID	4.64	4.55	3.8	3.39	3	n.d.	4.29	2.54	3.14	3.08	2.54	2.55	n.d.	n.d.	n.d.	n.d.
Rb MS-ID	2.62	0.5	0.59	0.32	0.52	0.56	3.92	1.28	6.1	1.19	0.75	1.08	10.54	2.44	1.27	1.17
Sr MS-ID	233	115	178	107	131	115	179	148	177	124	145	143	207.37	121	141	106
$^{87}Sr/^{86}Sr$	0.70264	0.70261	0.70257	0.70253	0.70255	0.702541	0.7029	0.703	0.70314	0.70293	0.70283	0.70346	0.703647	0.702837	0.702810	0.702849
$^{143}Nd/^{144}Nd$-1	0.513123	0.513058	0.513074	0.513139	0.513118	0.513054	0.513037	0.513007	0.512972	0.513036	0.513041	0.512978	0.512903	0.513298	0.513184	0.513234
ε_{Nd}	8.29	8.43	8.15	8.7	8.47	8.08	7.16	7.22	6.79	7.35	7.8	7.14	5.13	12.83	10.61	11.58
$^{143}Nd/^{144}Nd$-2	0.513065	0.513072	0.513058	0.513086	0.513074	n.d.	0.513007	n.d.	0.512988	0.513017	0.51304	0.513006	n.d.	n.d.	n.d.	n.d.
$^{206}Pb/^{204}Pb$	18.805	18.911	18.998	18.812	18.572	18.630	18.057	18.008	18.225	18.248	17.944	17.772	17.8884404	17.489	17.764	17.805
$^{207}Pb/^{204}Pb$	15.499	15.514	15.613	15.503	15.482	15.475	15.439	15.462	15.465	15.489	15.409	15.494	15.4898316	15.416	15.431	15.421
$^{208}Pb/^{204}Pb$	38.262	38.319	38.468	38.166	38.097	38.099	37.858	37.794	38.211	38.003	37.743	37.837	37.8365904	37.332	37.584	37.638
$^{176}Hf/^{177}Hf$	0.283107	0.283104	0.283091	0.283129	0.283146	0.283160	0.283134	0.28314	0.283114	0.28311	0.283115	0.283163	0.283094	0.283589	0.283437	0.283417
ε_{Hf}	11.85	11.73	11.27	12.61	13.24	13.70	12.79	13.01	12.08	11.95	12.13	13.83	11.39	28.9	23.5	22.8

[a] Major elements are reported as weight percent, and trace elements are reported as parts per million; n.d. indicates that no data are available. Trace elements labeled "MS-ID" are measured by isotope dilution mass spectrometry. Data other than oxygen isotope data are from Klein et al. [1988, 1991], Pyle et al. [1992, 1995], Kempton et al. [2002], and Hanan et al. [2004]. Nd isotopic compositions measured in the same samples and reported in two different publications are reproduced here: $^{143}Nd/^{144}Nd$-1 [Klein et al., 1988] and $^{143}Nd/^{144}Nd$-2 [Kempton et al., 2002].
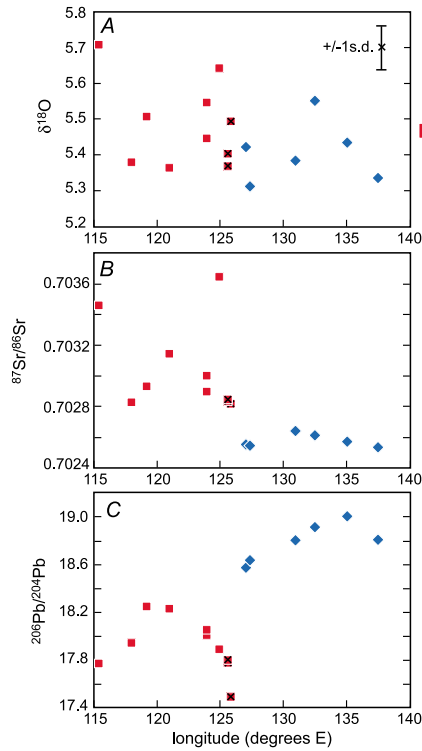

Figure 1. (a) Oxygen isotope composition versus longitude, (b) $^{87}Sr/^{86}Sr$ versus longitude, and (c) $^{206}Pb/^{204}Pb$ versus longitude of AAD samples used in this study, illustrating the distinctions in Sr and Pb isotopic composition between Indian- and Pacific-type MORB at the AAD. Indian-type samples are shown with red squares (zone B4 samples are shown with red squares with black crosses), and Pacific-type samples are shown with blue diamonds; sample classification is based on *Pyle et al.* [1992, 1995]. Average reproducibility of replicate measurements of the same samples (1 s.d.) is shown in Figure 1a. Average values of $\delta^{18}O$ (±2 times the standard error of the mean) of the Indian- and Pacific-type samples are shown by large symbols to the right of the diagram in Figure 1a. See section 4.1 for discussion.

sections 4.1.1–4.1.4, we examine the constraints that oxygen isotope compositions can place on the presence of each of the four types of materials proposed to have influenced the chemical composition of Indian upper mantle.

4.1.1. Pelagic Sediment

[10] One explanation for the low $^{206}Pb/^{204}Pb$ in Indian MORB compared to Pacific or Atlantic MORB is that a small amount of pelagic sediment has been added to the upper mantle in the Indian basin compared to the Pacific or Indian upper mantle [e.g., *Rehkämper and Hofmann*, 1997]. Pelagic sediment has very high $\delta^{18}O$ (20–40‰) compared to upper mantle compositions (~5.5‰)
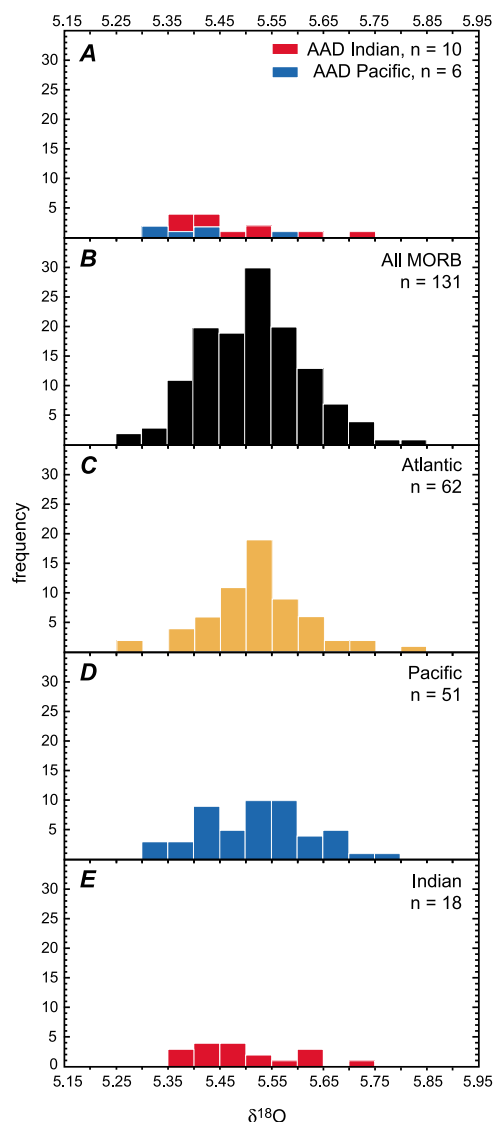
Figure 2. Histograms of $\delta^{18}O$ for MORB samples. All data are high-precision, laser fluorination measurements of fresh MORB glasses. (a) AAD samples (this study). (b) Compilation of all available high-precision $\delta^{18}O$ data: AAD data from this study, previously published results for the mid-Atlantic ridge and N-MORB data [*Cooper et al.*, 2004; *Eiler et al.*, 2000b], and East Pacific Rise data from the Caltech laboratory (Table S1). (c) Subset of the data in Figure 2b, including only Atlantic MORB. (d) Subset of the data in Figure 2b, including only Pacific MORB. (e) Subset of the data in Figure 2b, including only Indian MORB.

and therefore addition of even small amounts of pelagic sediment to the Indian MORB source should lead to systematically higher $\delta^{18}O$ in Indian MORB than in Pacific or Atlantic MORB. If, for example, there is approximately 1% of pelagic sediment in the Indian upper mantle

[e.g., *Rehkämper and Hofmann*, 1997] that is not present in the Pacific upper mantle, with $\delta^{18}O$ of ~20‰ [*Eiler*, 2001], then the average $\delta^{18}O$ of I-MORB should be 0.15‰ higher than average Pacific MORB. This difference is small in absolute terms, but is approximately four times the standard error of our measured average values for each ocean basin suite, and so should be easily observed. The lack of a measurable distinction between average $\delta^{18}O$ of Indian and Pacific MORB in the AAD (Figure 1) therefore argues against an origin for Indian MORB by addition of pelagic sediment. This conclusion is also consistent with arguments against a significant proportion of pelagic sediment in the I-MORB source based on Hf isotopic compositions and $\delta^{18}O$ in NMORB samples [*Eiler et al.*, 2000b; *Hanan et al.*, 2004; *Janney et al.*, 2005].

4.1.2. Enriched Mantle Associated With Local Plumes

[11] Another potential source of enriched material in the Indian upper mantle is contamination of the upper mantle by the same enriched component responsible for the more enriched radiogenic isotopic compositions of local oceanic island basalts (OIB) or the Kerguelen plateau. For example, *Pyle et al.* [1995] suggest that material related to the Kerguelen plume was dispersed in the Indian upper mantle near the AAD during an increase in spreading rate. In addition, *Rehkämper and Hofmann* [1997] attribute some of the second-order scatter in the Pb isotopic data to small but variable amounts of a component related to Indian Ocean OIB, although they also argue that the known Indian Ocean OIB lavas have Pb isotopic signatures that are too radiogenic to explain the first-order geochemical differences between I-MORB and P-MORB. Oxygen isotope signatures of most OIB are similar to those of normal MORB with the exception of EM2-type OIB, which range to significantly higher $\delta^{18}O$ than NMORB [*Eiler et al.*, 1997; *Workman et al.*, 2008]. Kerguelen plume material is EM-1 type, similar in $\delta^{18}O$ to N-MORB [*Eiler et al.*, 1997] and therefore oxygen isotope composition is not diagnostic of the presence (or absence) of local plume material. HHowever, we note that the two samples of I-MORB with the highest $\delta^{18}O$ also have the highest $^{87}Sr/^{86}Sr$ and $^{207}Pb/^{204}Pb$ ratios of the AAD samples, associations also noted by *Eiler et al.* [1997] and *Workman et al.* [2008] for EM-2 type OIB. One of the two (MW8801-027-058) has consistently enriched isotopic and trace element signatures, with the lowest

ε_{Nd} and ε_{Hf} of the AAD samples, and high K_2O and $(La/Sm)_N$, whereas the other (D10-10) has similar ε_{Hf} and ε_{Nd} to the majority of AAD samples. Therefore, these two samples may reflect similar processes to those that produced EM2-type OIB sources, such as the local presence of recycled oceanic crust including very small amounts of recycled sediment, sediment-derived fluids or melts [e.g., *Eiler et al.*, 1997; *White and Hofmann*, 1982], as a small-scale heterogeneity superimposed on the first-order distinction between Indian- and Pacific-type upper mantle.

4.1.3. Subduction-Modified Mantle

[12] *Gurnis et al.* [1998] proposed a dynamical model in which the depth anomaly, westward migration of the isotopic boundary, and the distinctive crustal thickness of the AAD reflect the presence of a slab that stagnated in the transition zone during Cretaceous subduction and has since been drawn up toward the surface by spreading at the Southeast Indian Ridge. *Kempton et al.* [2002] argue on the basis of Hf-Nd isotope systematics that subduction-modified mantle above this slab is responsible for the distinctive isotopic characteristics of I-MORB at the AAD and potentially elsewhere in the Indian basin. *Hanan et al.* [2004], on the other hand, argue against this model for the origin of Indian MORB mantle on the basis of high $^3He/^4He$ and low $^{206}Pb/^{204}Pb$ in I-MORB at the AAD, and *Christie et al.* [2004] argue that the model requires a source that is too old and too widespread to be derived from Cretaceous subduction. Our results qualitatively support the *Hanan et al.* [2004] and *Christie et al.* [2004] interpretation, although we cannot definitively rule out the influence of slab-derived fluids on the basis of oxygen isotopes. For example, based on studies of $\delta^{18}O$ in mafic arc lavas, inferred $\delta^{18}O$ of slab-derived components (whether aqueous fluids or water-rich silicate melts) are similar to those of the oceanic sediment or altered oceanic crust from which they are derived [e.g., *Eiler et al.*, 2000a, 2005; *Macpherson et al.*, 1998]. Thus, fluid-rock interactions in the mantle beneath arcs appear not to strongly fractionate oxygen isotopes, and fluid released from a stranded slab at higher temperatures would be expected to have even smaller fractionations between fluid and residue. Therefore, metasomatic fluids derived from the slab would likely have $\delta^{18}O$ similar to that of the slab, i.e., $\delta^{18}O$ higher than ambient mantle if the fluids are derived from the upper oceanic crust, and lower than ambient mantle if derived from the lower

crustal section [e.g., *Alt and Teagle*, 2000; *Eiler*, 2001]. As a result, consistent with the results of modeling fluid addition beneath arcs [e.g., *Eiler et al.*, 2000a, 2005; *Macpherson et al.*, 1998], any hydrous or silicate fluid present in mass fractions sufficient to explain the trace element and isotopic distinctions between Indian- and Pacific-type MORB would likely also carry enough mass of oxygen to significantly change the average $\delta^{18}O$ of Indian MORB compared to Pacific-type MORB (unless there was a fortuitous balance between fluids derived from the upper and lower crustal section). Nevertheless, the presence of a small amount of metasomatic fluid may be consistent with the range of $\delta^{18}O$ observed in our results. Furthermore, the effects of subduction processing on the isotopic and trace element characteristics of altered oceanic crust are not fully understood; therefore, it is possible that subduction-processed oceanic crust could have characteristics somewhat different from those inferred above. Therefore, whereas our data qualitatively support the interpretations of *Hanan et al.* [2004] and *Christie et al.* [2004] that subduction-modified mantle is unlikely to be the source of the isotopic distinctions between I-MORB and P-MORB at the AAD, the oxygen isotope data alone do not make a strong case against fluid-modified mantle.

4.1.4. Continental Lithospheric Mantle or Lower Crust

[13] Another potential explanation for the distinctions between Indian and Pacific MORB is that the Indian depleted upper mantle is contaminated with subcontinental lithospheric mantle [e.g., *Goldstein et al.*, 2008; *Hawkesworth et al.*, 1986; *Mahoney et al.*, 1991] or lower continental crust [e.g., *Escrig et al.*, 2004; *Hanan et al.*, 2004; *Janney et al.*, 2005]. Most xenoliths derived from subcontinental lithospheric mantle (SCLM), whether anhydrous or hydrated, span a relatively narrow range of $\delta^{18}O$ (5.5 ± 0.2‰) [*Eiler*, 2001, and references therein; *Mattey et al.*, 1994] indistinguishable from the mantle source(s) of NMORB, and therefore if the enriched isotopic signature of Indian MORB were due to contamination of depleted upper mantle with enriched SCLM, we would predict that there would be no correlation between $\delta^{18}O$ and radiogenic isotope indices of enrichment. The fact that we do observe correlations between $\delta^{18}O$ and enriched radiogenic isotope signatures (e.g., $^{87}Sr/^{86}Sr$ and $^{207}Pb/^{204}Pb$ (Figure 3)), in our results argues against the notion that SCLM is the dominant enriched component present in the mantle
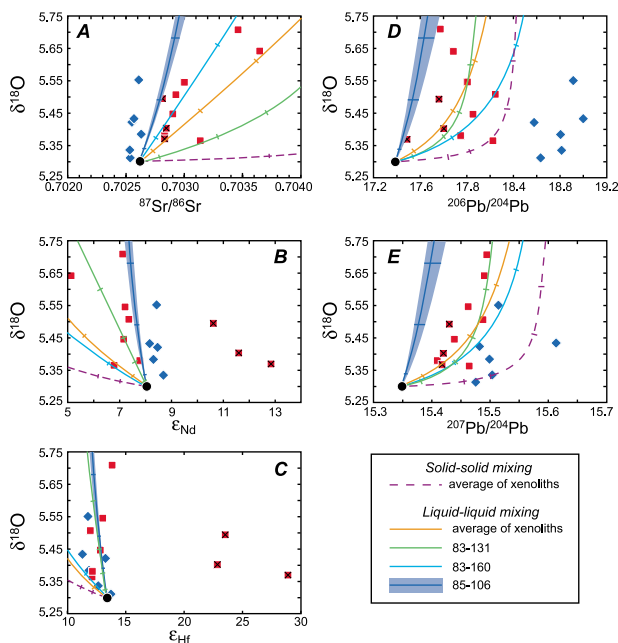
Figure 3. Oxygen isotope composition of AAD samples versus (a) $^{87}Sr/^{86}Sr$, (b) ε_{Nd}, (c) ε_{Hf}, (d) $^{206}Pb/^{204}Pb$, and (e) $^{207}Pb/^{204}Pb$. Sources for data other than oxygen isotope compositions are listed in Table 1. Symbols are as in Figure 1. Also shown are results for mixing calculations between depleted mantle (black circle) and Australian lower crustal xenoliths. Dashed line indicates a solid-solid mix of depleted mantle with an average of the lower crustal xenoliths (Table 2); tick marks indicate 0.5%, 1%, 5%, and 10% xenoliths in the source. Other lines indicate mixes of 5% partial melt of DMM with 20% partial melts of individual xenoliths or the average of Australian lower crustal xenoliths; the shaded bands around the curves for xenolith 85-106 show the effects of changing the degree of partial melting of the xenoliths to 10% or 30%. Tick marks along curves indicate 1%, 5%, 10%, and (where within the range of the diagrams) 20% of the melt derived from xenoliths. See section 4.2 for discussion.

sources of AAD I-type samples, a conclusion that is also supported by Os isotopic compositions of Indian MORB samples [*Escrig et al.*, 2004].

[14] More recently, *Hanan et al.* [2004] and *Escrig et al.* [2004] proposed a model, based on Hf-Nd-Pb isotopic compositions and Os isotopic compositions, respectively, of Indian MORB samples, in which the I-MORB source is depleted mantle that has been contaminated by lower continental crust that was entrained into the Indian upper mantle during the breakup of Gondwana. *Hanan et al.* [2004] also observe extremely high ε_{Hf} compared to the global MORB Hf-Nd array in a few of the AAD samples ("ultradepleted" samples) with ε_{Nd} that is relatively high compared to other local

Indian MORB samples (but not unusually high compared to the global array), such that that in plots of $^{206}Pb/^{204}Pb$ versus ε_{Hf} and ε_{Nd}, the low-$^{206}Pb/^{204}Pb$ end of the Indian MORB array is distinct from that of the Pacific array in Hf but not in Nd isotopic composition. *Hanan et al.* [2004] argue that this contrast in behavior between Hf and Nd is due to partial melting of some of this lower crustal contaminant during rifting, yielding a residue which evolved to very high ε_{Hf} (but not much higher ε_{Nd}) in the ~50 Ma since rifting. Thus, in this model, the enriched component contributing to the local I-type AAD MORB array (as defined by radiogenic isotopes) represents contamination of ambient depleted mantle by unmelted lower crust, whereas the depleted component represents ambient depleted mantle, and a third ("ultradepleted") component, distinguished by very high ε_{Hf}, represents residues of earlier partial melting of the enriched component mixed with ambient depleted mantle. *Janney et al.* [2005] also addressed the question of the origin of Indian-type MORB source using Nd, Hf, and Pb isotopic compositions and trace element patterns of Southwest Indian Ridge basalts. Their favored model is that Indian-type mantle reflects incorporation of ancient subcontinental lithospheric mantle or lower continental crust during the breakup of Gondwana.

[15] The combined oxygen and radiogenic isotope characteristics of lower crustal xenoliths are qualitatively consistent with the *Hanan et al.* [2004] and *Escrig et al.* [2004] model for the origin of the AAD Indian-type MORB mantle. For example, measurements of lower crustal xenoliths from Australia (used by *Hanan et al.* [2004] as an analog for lower crust in the Indian upper mantle) suggest that Gondwanan lower crust was heterogeneous in $\delta^{18}O$, but generally enriched in ^{18}O relative to MORB ($\delta^{18}O$ of 6.2 to 13.5‰ [*Kempton and Harmon*, 1992]). It is also likely that this ancient lower crust would have elevated $^{207}Pb/^{204}Pb$ relative to $^{206}Pb/^{204}Pb$ compared to oceanic mantle [e.g., *Hofmann*, 2003]. The Australian lower crustal xenoliths have these characteristics, with variable but relatively radiogenic Sr and Pb (especially $^{207}Pb/^{204}Pb$) and unradiogenic Nd and Hf isotopic compositions (Table 2) [*Kempton and Harmon*, 1992; *Rudnick*, 1990; *Rudnick and Goldstein*, 1990; *Vervoort et al.*, 2000]. Partial melting calculations by *Eiler* [2001] show that, at least with melting of spinel peridotite in the presence of residual olivine, melting extents in the normal range for MORB will shift $\delta^{18}O$ in the melt by less than ~0.1‰ while the residue shifts by less

Table 2. Compositions of Australian Lower Crustal Xenoliths and Model Depleted Mantle Used in Mixing/Melting Calculations[a]

	$\delta^{18}O$	Sr (ppm)	$^{87}Sr/^{86}Sr$	Nd (ppm)	$^{143}Nd/^{144}Nd$	ε_{Nd}	Pb (ppm)	$^{206}Pb/^{204}Pb$	$^{207}Pb/^{204}Pb$	Hf (ppm)	$^{176}Hf/^{177}Hf$	ε_{Hf}
				Average, Maximum, and Minimum of Data for Australian Lower Crustal Xenoliths (n = 22)								
Average	8.4	306.4	0.709199	10.8	0.512444	−3.78	2.6	18.5	15.6	3.0	0.282774	0.06
Maximum	13.2	589.9	0.723648	27.5	0.513126	9.52	11.8	19.2	15.7	19.0	0.283208	15.4
Minimum	6.2	39.3	0.702390	1.5	0.511724	−17.8	0.3	17.8	15.5	0.1	0.282100	−23. 8
				Example Australian Lower Crustal Xenoliths								
83-131	6.8	415.3	0.70519	2.26	0.512594	−0.86	2.05	18.15	15.52	0.33	0.282962	6.72
83-160	12.5	203	0.715103	24.4	0.51228	−6.98	8.2	18.82	15.62	4.2	0.282668	−3.68
85-106	9.1	164	0.703928	11.2	0.512964	6.36	0.3	18.27	15.53	2.21	0.283062	10.3
				Depleted Mantle Compositions								
D-DMM	5.25	6.092	0.70219	0.483	0.51326	12.1	0.014	17.573	15.404	0.127	0.28350	25.7
DMM	5.50	7.664	0.70263	0.581	0.51313	9.56	0.018	18.275	15.486	0.157	0.28326	17.3
E-DMM	5.75	9.718	0.70307	0.703	0.513	7.02	0.024	18.977	15.568	0.186	0.28310	11.6
Modified DMM	5.25	7.664	0.70263	0.581	0.51305	8.00	0.018	17.4	15.35	0.157	0.28315	25.7

[a] The $\delta^{18}O$ of Australian xenoliths is from *Kempton and Harmon* [1992]. Sr-Nd data for xenoliths are from *Rudnick* [1990], Pb data are from *Rudnick and Goldstein* [1990], and Hf data are from *Vervoort et al.* [2000]. Depleted mantle compositions are from *Workman and Hart* [2005]; "Modified DMM" composition is based on *Workman and Hart* [2005] DMM composition, with Nd and Pb isotopic compositions adjusted to fit the depleted end of the AAD Indian MORB array. Oxygen isotope composition of DMM is estimated based on the low end of the range of $\delta^{18}O$ in our AAD MORB data.

than the melt. Even at higher degrees of melting (up to 30%), the shift in $\delta^{18}O$ of the melt compared to the source is ∼0.15‰ [*Eiler*, 2001]. Therefore, compared to the variations of up to 7‰ in $\delta^{18}O$ between different lower crustal xenoliths [*Kempton and Harmon*, 1992], fractionations induced by partial melting will be small. Thus, both the enriched and "ultradepleted" components (and any melts produced from them) would largely retain their original oxygen isotope signatures.

[16] The lower crustal contamination model would therefore predict high $^{207}Pb/^{204}Pb$ relative to $^{206}Pb/^{204}Pb$, high $^{87}Sr/^{86}Sr$, and low $^{143}Nd/^{144}Nd$ associated with high $\delta^{18}O$ as the proportion of lower crustal material present in the MORB source increases, but would predict little to no correlation between $\delta^{18}O$ and low ε_{Hf} or ε_{Nd} values for the "ultradepleted" samples. All of these predictions are consistent with our results (Figure 3). The AAD IMORB samples that we measured include some of the "ultradepleted" samples of *Hanan et al.* [2004] (the zone B4 samples in Figures 1 and 3), as well as some of the most isotopically enriched samples in Indian-type AAD MORB, allowing us to explore this hypothesis in more detail. Within our AAD Indian-type samples, we observe a good correlation of high $\delta^{18}O$ with high $^{207}Pb/^{204}Pb$ (Figure 3). Plots of other radiogenic isotopic patterns versus $\delta^{18}O$ show more scatter, but the two samples with highest $\delta^{18}O$ also have high

$^{87}Sr/^{86}Sr$ and low ε_{Nd}, and have moderate to high $^{206}Pb/^{204}Pb$ and $^{208}Pb/^{204}Pb$ (Figure 3), all consistent with a relatively enriched trace element signature over geologic time. In contrast, ε_{Hf} in one of the samples with highest $\delta^{18}O$ is not unusually unradiogenic compared to the other samples in the suite (no Hf isotopic measurements are available for the other of the two highest-$\delta^{18}O$ samples). The zone B4 AAD samples (the "ultradepleted" samples of *Hanan et al.* [2004]) are not distinctive in their oxygen isotope compositions compared to the rest of the Indian-type AAD samples, although they do have high ε_{Nd} and low $^{87}Sr/^{86}Sr$, and generally fall in the unradiogenic end of the range in Pb isotope compositions (Figure 3).

[17] We can further test the lower crustal contamination model by calculating MORB compositions that would be produced by melting mixtures of depleted and enriched sources. Although the isotopic end-members appear to be qualitatively suitable to reproduce the range in the data, modeling of solid-solid mixing between Australian xenolith compositions and depleted MORB mantle (DMM) yields mixing hyperbolae that are in general too strongly curved to pass through the array of AAD I-MORB data (Figure 3). This is not surprising, as it would imply that the enriched and depleted components contributed to the melt in such a way as to maintain the original ratio of trace element concentrations in depleted and

enriched sources, essentially equivalent to assuming that the two components contribute to the melt in proportion to their abundance in the mixed source, and that each had similar bulk partition coefficients for all of the trace elements of interest. On the other hand, if we assume that the enriched component (i.e., the lower crustal material) melts to a higher degree than the depleted component, a reasonable assumption given the generally lower liquidus temperatures of crustal rocks compared to depleted mantle peridotite [e.g., *Hirschmann and Stolper*, 1996; *Kogiso et al.*, 2003, 2004; *Pertermann and Hirschmann*, 2003], then mixing of melts derived from depleted and enriched components can produce a satisfactory fit to the data arrays (Figure 3). Of course, given the heterogeneity in composition of the lower crust (as exemplified by the Australian lower crustal xenoliths), the assumption of a single composition for the enriched end-member is a simplification, and it is equally likely that the data arrays reflect differences in the specific enriched compositions present in the source of each MORB sample. Therefore, the calculations shown in Figure 3 use several xenoliths of varying composition as end-members. Similarly, the calculations shown in Figure 3 are based on 5% melting of the depleted mantle and 20% melting of the lower crustal xenoliths. This assumption is based on the estimate of average MORB production from DMM by ∼6% melting [*Workman and Hart*, 2005], and on a higher degree of melting of the lower crustal xenoliths, following previous work exploring the consequences of a mixed peridotite-pyroxenite/eclogite source [e.g., *Elkins et al.*, 2008; *Hirschmann and Stolper*, 1996; *Kogiso et al.*, 2004; *Pertermann and Hirschmann*, 2003; *Reiners*, 2002; *Stracke et al.*, 1999]. Changing the melt fraction for the enriched component between 10 and 30% has a minor effect on the position of each curve relative to the range of solutions using different xenolith compositions (Figure 3), and therefore does not change our conclusions. However, because of the uncertainties in the exact composition and degree of melting of the end-members, the calculations shown in Figure 3 are intended to be illustrative rather than to uniquely constrain the percentage of melting or exact composition of each end-member. Furthermore, given the small number of samples, we do not attempt to model the "ultradepleted" samples in detail, but simply note that their oxygen and radiogenic isotopic characteristics are qualitatively consistent with the model proposed by *Hanan et al.* [2004]. Nevertheless, these calculations do illustrate that the presence of lower crustal material

distributed within the upper mantle which has compositions within the range of those of lower crustal xenoliths can explain the combined oxygen isotopic and radiogenic isotopic characteristics of the AAD I-MORB source.

[18] We can add to the lower crustal contamination model of *Hanan et al.* [2004] and *Escrig et al.* [2004] by estimating the percentage of lower crustal material present in the AAD I-MORB source, albeit with some uncertainties imposed as a result of the heterogeneity of oxygen isotope composition of the lower crust. For example, higher $\delta^{18}O$ in MORB could reflect either a higher percentage of lower crust present in the melting zone, or a higher $\delta^{18}O$ in the local lower crustal contaminant within the melting zone for different samples. However, the problem is simplified by the fact that depleted and enriched components will have roughly the same abundance of oxygen, so that mixing calculations reflect the relative proportion of melt contributed by each source. Given this, we can place some limits on the amount of lower crust present by examining the range of $\delta^{18}O$ in AAD I-type samples compared to the range of $\delta^{18}O$ measured in Australian xenoliths. For example, assuming that the lowest-$\delta^{18}O$ AAD MORB samples (at ∼5.30‰) represent uncontaminated ambient depleted mantle and assuming that the lower crustal contaminant has $\delta^{18}O$ of 8.4‰ (the average of the Australian xenoliths), the AAD sample with the highest $\delta^{18}O$ would be composed of a mixture of 13% melt originating from the lower crustal contaminant with 87% of the melt originating from the depleted mantle. If the enriched and depleted mantle partially melted to different degrees, with 10–20% melting of the enriched component and 5% melting of the depleted component, this proportion would imply that the upper mantle prior to melting contained 5–7% lower crust. Assuming instead the highest and lowest $\delta^{18}O$ of the Australian xenoliths for the lower crustal contaminant (13.2‰ and 6.2‰, respectively) yields 5 or 45% melt from lower crust, respectively, corresponding to ∼1–3% or 17–29%, respectively, lower crust in the unmelted upper mantle. These calculations are consistent with the estimate of 4–15% recycled lower crust in the Indian upper mantle based on Os isotopes [*Escrig et al.*, 2004]. Although there is a contribution to uncertainty in our calculations due to the choice of $\delta^{18}O$ for the model depleted mantle (5.3‰), it is unlikely that depleted mantle would have $\delta^{18}O$ significantly lower than 5.25‰ (the lowest measured in fresh MORB measured to

date); therefore, the choice of $\delta^{18}O$ for the depleted component has little effect on these calculations.

[19] Therefore, we conclude that contamination of the Indian upper mantle by heterogeneous old continental lower crust can explain the radiogenic isotope and oxygen isotope characteristics of AAD Indian-type MORB. Based on the range of $\delta^{18}O$ of lower crust seen in the Australian xenoliths compared to that measured in AAD Indian-type MORB, we estimate that the Indian-type upper mantle at the AAD contains on average a few percent of enriched material derived from lower continental crust in addition to whatever percentage may be present in the Pacific-type AAD. Furthermore, the heterogeneity of the lower crust is consistent with more diverse radiogenic isotope compositions in Indian-type compared to Pacific-type AAD MORB.

4.2. Global Variations of $\delta^{18}O$ in MORB

### 4.2.1. Observations From Laser Fluorination Data

[20] Although more restricted in composition and in general more depleted than oceanic island basalts (OIB), the mantle sources of MORBs have long been recognized to be heterogeneous in trace element and radiogenic isotopic composition [e.g., *Cohen et al.*, 1980; *Dupre and Allegre*, 1983; *Hart*, 1971, 1984; *Hofmann*, 2003, and references therein; *Salters and Stracke*, 2004; *Schilling et al.*, 1983; *Tatsumoto et al.*, 1965; *Workman and Hart*, 2005]. This heterogeneity has been attributed to small amounts of trace element-enriched material distributed throughout the ambient, depleted, upper mantle. However, the origin and abundance of this enriched material is difficult to constrain, partly due to the difficulty of deconvolving the effects of parent-daughter fractionation and aging on radiogenic isotope ratios. The variations in $\delta^{18}O$ of fresh MORB provide additional information on the nature of this enriched component or components, and in particular, allow us to better estimate the abundance of enriched material. Comparisons between $\delta^{18}O$ and trace element and radiogenic isotope characteristics of MORB have been examined before, and have found either no or weak correlations in the global data set [*Harmon and Hoefs*, 1995; *Ito et al.*, 1987]. However, correlations between $\delta^{18}O$ and trace element characteristics of MORB have been observed in some high-precision, geographically or compositionally restricted data sets [e.g., *Cooper et al.*, 2004; *Eiler*

et al., 2000b]; therefore, it is worth reexamining the global MORB data set. We have compiled a data set of high-precision laser fluorination measurements of $\delta^{18}O$ in MORB (those published by *Cooper et al.* [2004] and *Eiler et al.* [2000b], plus additional samples from this study (Tables 1 and S1)). Our goal with this compilation is to revisit the question of whether global variations in $\delta^{18}O$ of MORB are correlated with other geochemical indices of enrichment, and if so, to what extent the variations reflect the physical distribution of heterogeneities within the upper mantle, rather than to further examine the causes of such mantle heterogeneity.

[21] Although there is a range in $\delta^{18}O$ within samples of MORB from each ocean basin, data for each ocean basin show remarkably similar distributions (Figure 2). Oxygen isotope data for each ocean basin fit a normal distribution, with statistically indistinguishable means and standard deviations (Pacific: $\mu = 5.52‰$, $\sigma = 0.11$; Atlantic: $\mu = 5.52‰$, $\sigma = 0.10$; and Indian: $\mu = 5.50‰$, $\sigma = 0.10$) and with a total range of $\delta^{18}O$ of ~ 5.25–5.8‰. The similarity between the mean of the distribution for each ocean basin was confirmed by two-sample t tests comparing pairs of data sets, which indicate indistinguishable means for all of the data sets at the 95% confidence level. The standard error of the mean of replicate measurements of $\delta^{18}O$ for these samples is significant compared to the standard deviation of each data set (average of 0.03‰ compared to 0.1‰); however, despite the fact that analytical error undoubtedly introduces some scatter to the data sets, it can account for only a third of the total variance. These characteristics suggest that (1) variations in $\delta^{18}O$ in MORB are not the result of analytical uncertainty alone (a conclusion which is supported by the correlations of $\delta^{18}O$ with other geochemical indices of enrichment in NMORB [*Eiler et al.*, 2000b], MAR [*Cooper et al.*, 2004], and AAD data (this study)); (2) variations in $\delta^{18}O$ in MORB from all ocean basins reflect some stochastic process, resulting in a normal distribution; and (3) whatever process leads to variations in $\delta^{18}O$ in fresh MORB, it appears to operate consistently across all ocean basins.

[22] In general, variations in $\delta^{18}O$ of MORB can be attributed to four possible causes: (1) posteruptive alteration; (2) shallow level differentiation, including contamination and fractional crystallization; (3) partial melting processes; and (4) heterogeneity in $\delta^{18}O$ of the mantle source. Of these, the first is
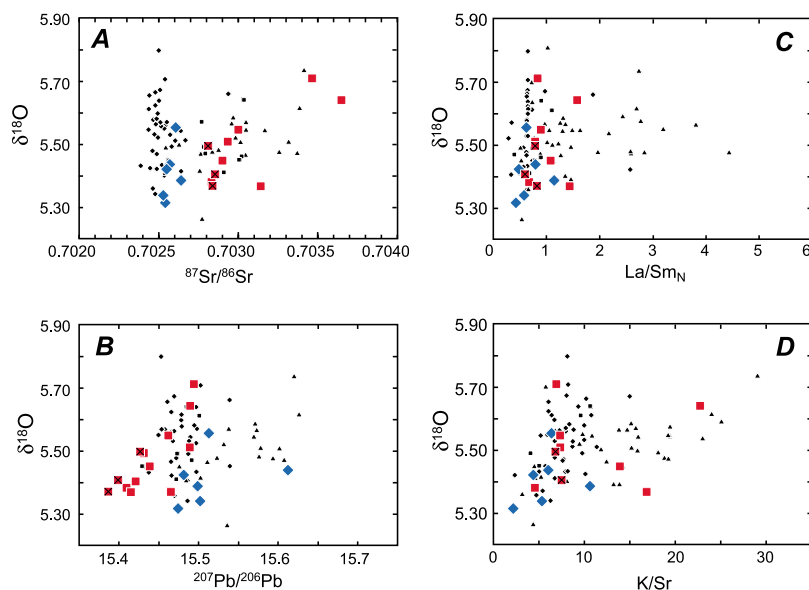
Figure 4. Oxygen isotope composition of samples in global high-precision MORB compilation versus (a) $^{87}Sr/^{86}Sr$, (b) $^{207}Pb/^{204}Pb$, (c) chondrite-normalized La/Sm ratio, and (d) K/Sr. Symbols for AAD samples (this study) are as in Figures 1 and 3. Other data are Pacific MORB (black diamonds), Atlantic MORB (black triangles), and Indian MORB (black squares). Data other than AAD samples are from previously published results for the mid-Atlantic ridge and N-MORB data [*Cooper et al.*, 2004; *Eiler et al.*, 2000b], and East Pacific Rise data are from the Caltech laboratory (oxygen isotope data are given in Table S1; radiogenic isotope and trace element data for the samples shown are from *Eiler et al.* [2000b], *Sims et al.* [2002, 2003], *Cooper et al.* [2004], and *Schiano et al.* [1997, and references therein]).

contraindicated by several factors: all samples analyzed were fresh, hand-picked glass, and correlations of $\delta^{18}O$ with indicators of seawater-basalt interaction (for example, Cl content or high $^{87}Sr/^{86}Sr$ without accompanying changes in $^{143}Nd/^{144}Nd$) are absent [e.g., *Cooper et al.*, 2004; *Eiler et al.*, 2000b]. Changes in $\delta^{18}O$ during fractional crystallization and differentiation in a crustal magma reservoir [*Cooper et al.*, 2004] and during partial melting of a homogeneous source [*Eiler*, 2001] are both expected to produce variations in $\delta^{18}O$ of less than ~0.1‰, and are therefore unlikely to exert a first-order control on the variations of $\delta^{18}O$ in the MORB database. Furthermore, there is a broad association of $\delta^{18}O$ globally with "enriched" signatures in trace element and radiogenic isotopic data (e.g., La/Sm, $^{87}Sr/^{86}Sr$, $^{207}Pb/^{204}Pb$ (Figure 4)). This observation indicates that $\delta^{18}O$ is correlated with measures of the proportion of an enriched mantle component in the MORB source, which in turn suggests that variations in $\delta^{18}O$ primarily reflect source heterogeneity.

[23] Nevertheless, partial melting processes potentially play a role in producing some of the heterogeneity observed in MORB, in that the partial melting response of enriched and depleted components under the same melting conditions will be somewhat different. For example, if there is some crustal material distributed within the upper mantle which differs from ambient depleted upper mantle in its bulk composition and mineralogy as well as its trace element and radiogenic isotopic characteristics, the degree to which it would be sampled during melting could potentially vary with changes in melt fraction, mantle temperature, and/or spreading rate along the global mid-ocean ridge system, which would in turn predict differences in trace element and isotopic indices of enrichment where melting parameters vary [e.g., *Allegre et al.*, 1984]. However, there is no systematic difference between $\delta^{18}O$ in subsets of the laser fluorination MORB data set based on degree of melting or spreading rate. For example, comparing the EPR/Siqueiros data set to the AAD data provides a test of the effects of fast versus slow spreading rates, and no systematic differences are apparent. The AAD also represents near-end-member values of cold mantle and low extents of melting (with associated trace element enrichments); compared to the rest of the global MORB data set they are unremarkable in $\delta^{18}O$. Therefore, we conclude that effects of partial melting processes and changes in spreading rate on sampling of enriched mantle domains cannot

account for the first-order variation within the global MORB $\delta^{18}O$ data.

4.2.2. Statistical Analysis of MORB Oxygen Isotope Data

[24] Given that the variations in $\delta^{18}O$ of MORBs appear primarily to reflect the abundance and distribution of enriched components in their mantle sources, the distribution of $\delta^{18}O$ in MORB should provide information about the underlying nature and distribution of upper mantle heterogeneities. Many earlier publications have used a statistical approach to examine mantle heterogeneity [e.g., *Albarede*, 2001; *Allegre et al.*, 1987; *Kellogg et al.*, 2002, 2007; *Meibom and Anderson*, 2004; *Prinzhofer et al.*, 1989; *Rudge et al.*, 2005] and the work presented here is conceptually similar in approach to many of these earlier studies in the sense of using forward modeling of sampling mantle heterogeneities to compare to geochemical data for ocean floor basalts. However, our work differs from earlier studies in that we focus on examining the distribution of isotopic compositions of a stable, major element (oxygen), which provides complementary information to that provided by radiogenic isotopes of trace elements. Furthermore, we focus on understanding the implications of the apparently normal distribution of $\delta^{18}O$ in each ocean basin, with identical means and standard deviations, on the distribution of enriched material in the mantle. This contrasts with previous work which focuses on radiogenic isotope and trace element distinctions between samples from different locations.

[25] For a given physical distribution of enriched and depleted components in the upper mantle and a given melting volume, a characteristic statistical distribution of data will be produced, with a mean that reflects the proportions and $\delta^{18}O$ values of enriched and depleted materials, and a standard deviation and skewness that reflect the sizes and spacing of those materials. In the following discussion, we refer to this characteristic statistical distribution as the "parent distribution." There are a number of possible types of parent distributions that could be appropriate descriptions of mantle heterogeneity. The physical distribution of heterogeneities within Earth's upper mantle and the melting process (the size of the melting regime and the relative degrees of melting of enriched and depleted domains) will both have an effect on the statistical distribution of data for a given isotopic system. Statistical distribution of oxygen isotopes

could be different from the distributions of radiogenic isotopes of trace elements due to the fact that trace elements will vary widely in abundance between enriched and depleted materials, whereas abundance of oxygen will be similar (~50 wt %) in all mantle rocks. Nevertheless, we can make some qualitative predictions of the expected distribution of $\delta^{18}O$ in MORB by analogy to the results of studies examining these type of effects on radiogenic isotope data. For example, *Kellogg et al.* [2002, 2007] examined Sr, Nd, and Pb isotopic data for MORB and OIB using a model in which enriched material was randomly distributed throughout the mantle, and randomly sampled by a melting volume (or melting area, in these 2-D simulations). Their model results predicted a variety of distributions of Nd isotopic data, ranging from a very narrow but symmetric distribution to a broader, skewed distribution, depending primarily on the length scale of mantle heterogeneities relative to the length scale of sampling (i.e., the region of partial melting beneath a ridge). In the case where the sampling length scale was large compared to the length scale of the heterogeneities, a normal distribution was produced, whereas skewed distributions were produced as the length scale of sampling decreased, because enriched mantle was in some cases able to more effectively dominate the Nd isotopic signature of the melt [*Kellogg et al.*, 2002]. In the case of randomly distributed enriched components within the upper mantle, we would expect a similar relationship to hold for oxygen isotopes, although the skewness and the overall range of data would likely be less than for Nd isotopic data because the roughly equal abundance of oxygen in mantle rocks of both enriched and depleted compositions leads to less effective leverage of the enriched component on the composition of the mixture than is the case for trace elements. However, the mean value would reflect the average percentage of enriched versus depleted component in the melt for a given $\delta^{18}O$ of each of the end-member compositions (and therefore, the percentage of each component present within the solid mantle, modified by the melt fraction of each component contributing to the melt).

[26] To our knowledge, the geochemical effects of sampling a nonrandom distribution of enriched material in the mantle have not been evaluated. Geodynamic simulations of mantle mixing often produce a range of behavior between efficient mixing (which leads to randomly distributed enriched material) and the preservation of layers or domains of substantial size [e.g., *Brandenburg*

et al., 2008; *Kellogg et al.*, 1999; *Xie and Tackley*, 2004]. If layers that are relatively large compared to the melting volume remain intact within the upper mantle, it is possible that the expected distribution of MORB oxygen isotope data might be skewed or even bimodal (if the sampling volume were small enough to sometimes sample essentially pure depleted or enriched components). Therefore, a better understanding of the extent to which the normal distribution of our compilation of $\delta^{18}O$ measurements in MORB reflects sampling a normal parent distribution may allow us to place constraints on the physical distribution of enriched material within the upper mantle.

[27] An additional factor to consider when using measured distributions of $\delta^{18}O$ to make inferences about the physical distribution of enriched and depleted domains within the mantle is that during analysis of MORB samples, some scatter is introduced to the data during the laser fluorination measurements themselves. Assuming that analytical error is random, this will tend to make the sample distribution more normal than the underlying distribution. Furthermore, the smaller the sample size of any given population, the more uncertainty there will be in using the statistical characteristics of the sample (mean, standard deviation, skewness) to estimate the shape (i.e., statistical characteristics) of the parent distribution. Therefore, our data (sample size of $\sim20-60$ data points per ocean basin) will be an imperfect representation of the oxygen isotope heterogeneity within the upper mantle. In order to determine how robust the estimates of shape of the parent distribution based on the MORB data are to the effects of limited sample size and analytical error, we performed Monte Carlo simulations by sampling parent distributions with a variety of means, standard deviations, and skewness, and adding synthetic "analytical error" to each sample data point. Our goal in this exercise was to falsify hypotheses (in the form of parent distributions with specific statistical characteristics) about the parent distribution in the mantle, thereby addressing the following questions: (1) How confident can we be that the data for different ocean basins were derived from similar parent distributions? (2) How different must the statistical parameters of a parent distribution be from the sample distribution in order to confidently eliminate it as a possible parent distribution for the MORB data?

[28] We performed two types of Monte Carlo simulations in order to address these questions.

First, we compared the actual measurements of $\delta^{18}O$ in MORB for each ocean basin to synthetic data generated for a range of parameters of the parent distribution, in order to determine which parameter combinations could be eliminated as possible parent distributions. These Monte Carlo simulations were set up to generate a synthetic data set through a random sample (n = 1000) of a parent distribution in the Pearson family. The sample size of 1000 was chosen in order to provide a data set that is representative of the parent distribution without being so large as to make the computations prohibitively slow; using sample sizes of 10,000 does not noticeably change the results but increases calculation time significantly. Each synthetic data point then had added to it "analytical error" in the form of a random sample of a normal distribution with mean of zero and standard deviation of 0.03‰ (equivalent to the standard error of the mean for replicate measurements, i.e., the average standard deviation (0.05‰) of replicate measurements of the same sample, divided by the square root of the average number of replicates), to generate the final synthetic data set. We used the standard error rather than the standard deviation of replicates in this exercise because this is a better metric to use when comparing data sets made up of data points which are themselves averages of several replicate measurements; however, our main conclusions from this exercise do not change if the "synthetic analytical error" is assumed to be 0.05‰, equivalent to the average standard deviation of replicate measurements of the same sample. Each synthetic data set was compared to the MORB data for each ocean basin using a two-sample Kolmogorov-Smirnov test, and the simulations repeated the process for each combination of parameters that defines a different parent distribution. We examined the following range of parameters for parent distributions: mean 5.35–5.65 (step size 0.005); standard deviation 0.01–0.29 (step size 0.005); skewness −1.2 to 1.2 (step size 0.3). Results are presented in Figures 5a–5c and Tables 3a–3d.

[29] The Kolmogorov-Smirnov test compares two data sets with the null hypothesis that they were both drawn from the same continuous distribution. The test result is 1 if the null hypothesis can be rejected at the 95% confidence level, and 0 if it cannot. Thus, in Figures 5a–5c, the regions shown in blue are those where the MORB data and the synthetic data are consistent with sampling the same underlying distribution, and the regions shown in red are where the MORB data and the synthetic data are inconsistent with sampling the
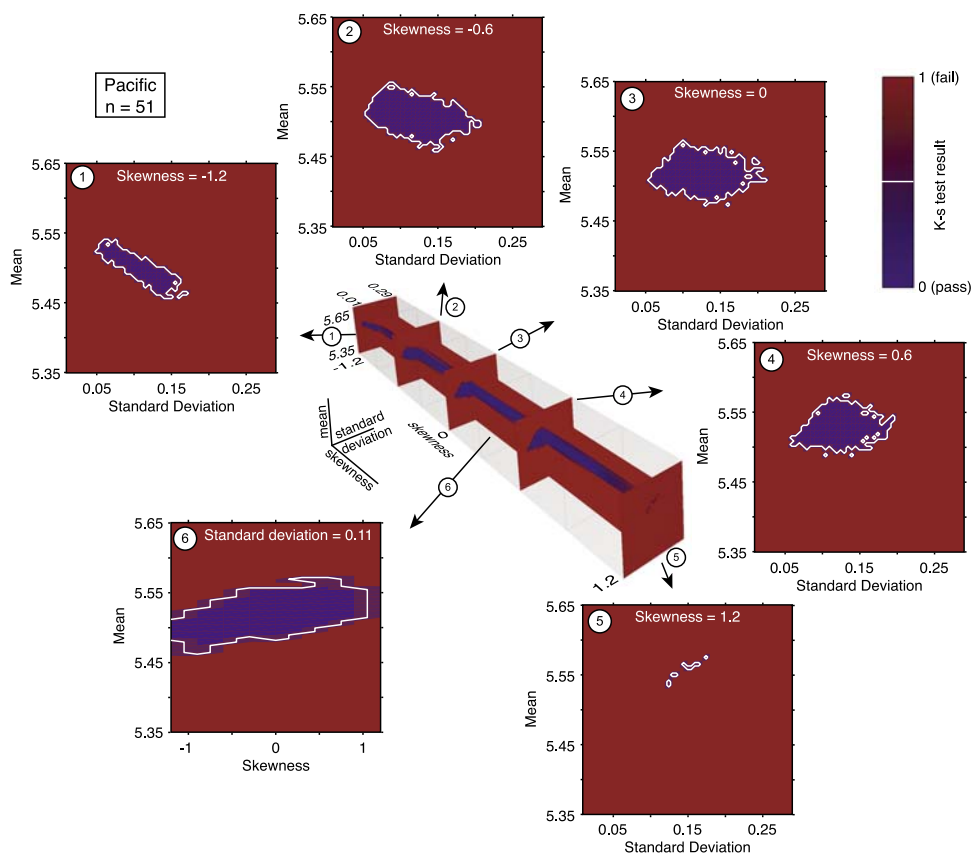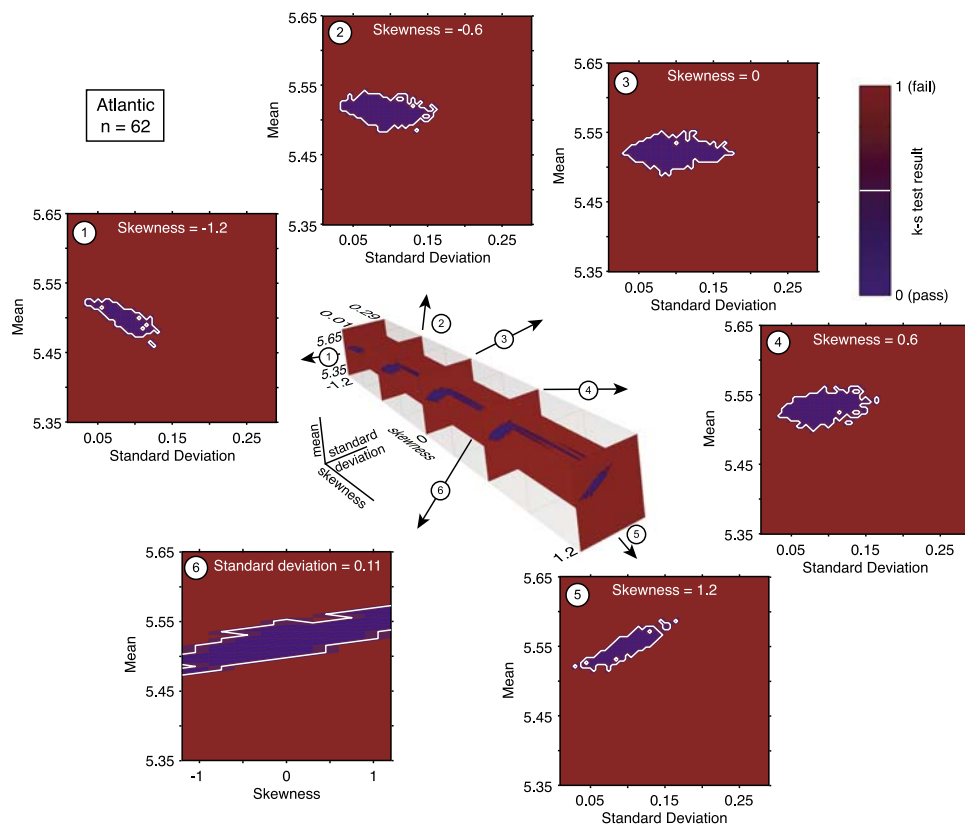
Figure 5a.   Diagrams showing results of Monte Carlo simulations comparing different parent distributions with data for Pacific MORB. Center shows a 3-D perspective view where the axes represent the range in mean, standard deviation, and skewness of the synthetic data sets used for comparison to the MORB data. Six slices of the data at constant skewness or standard deviation are shown in the 3-D perspective view and are also shown arrayed around the outside; arrows point from the slice locations on the 3-D view to the slices in 2-D. The synthetic data sets were generated by taking random samples (n = 1000) of a Pearson distribution with specific mean, standard deviation, and skewness (the parent distribution). Each of these synthetic data sets was compared to the MORB data using a two-sample Kolmogorov-Smirnov test, which returns a value of 0 if the two distributions compared are consistent with having been derived from the same parent data set and a value of 1 if they are not (at the 95% confidence level). Thus, blue areas represent parameter combinations which are potential parent distributions of the MORB data, whereas red areas represent parameter combinations which are not consistent with a parent distribution for the MORB data. The white contours represent a value of 0.5 and thus fall between grid points which can and cannot represent the parameters of the MORB parent distribution. Data analysis was performed using Visualizer 3-D [*Billen et al.*, 2008], a desktop visualization program which allows interaction with 3-D gridded data, for example, creating slices and isosurfaces and rotating and zooming in on the data in real time. The 3-D view is from a screen capture of a Visualizer 3-D session. See sections 4.2.2 and 4.2.3 for discussion.

same parent distribution (at the 95% confidence level). The results therefore map the region in parameter space which can (in red) and cannot (in blue) be eliminated as describing the parent distribution of the MORB data. For example, in the case of the data for the Pacific ocean (Figure 5a), if the underlying distribution is normal (i.e., skewness = 0) the mean and standard deviation of the parent distribution must be within the range 5.47–5.57‰ and 0.05–0.21, respectively (Table 3b). Furthermore, the mean and standard deviation trade off to some extent, where the range of acceptable mean values at very low standard deviation (close to 0.05) is much smaller than the acceptable range of mean values at moderate standard deviation (e.g., close to 0.1–0.15); in other words, the region of mean and standard deviations that are consistent with being the parent distribution for the Pacific MORB samples approximates an ovoid rather than a rectangle (Figure 5a). This applies to variations in skewness as well; at skewness both greater than and less than zero (i.e., nonnormal distributions), the region of acceptable parent distributions narrows in both mean and standard deviation, and
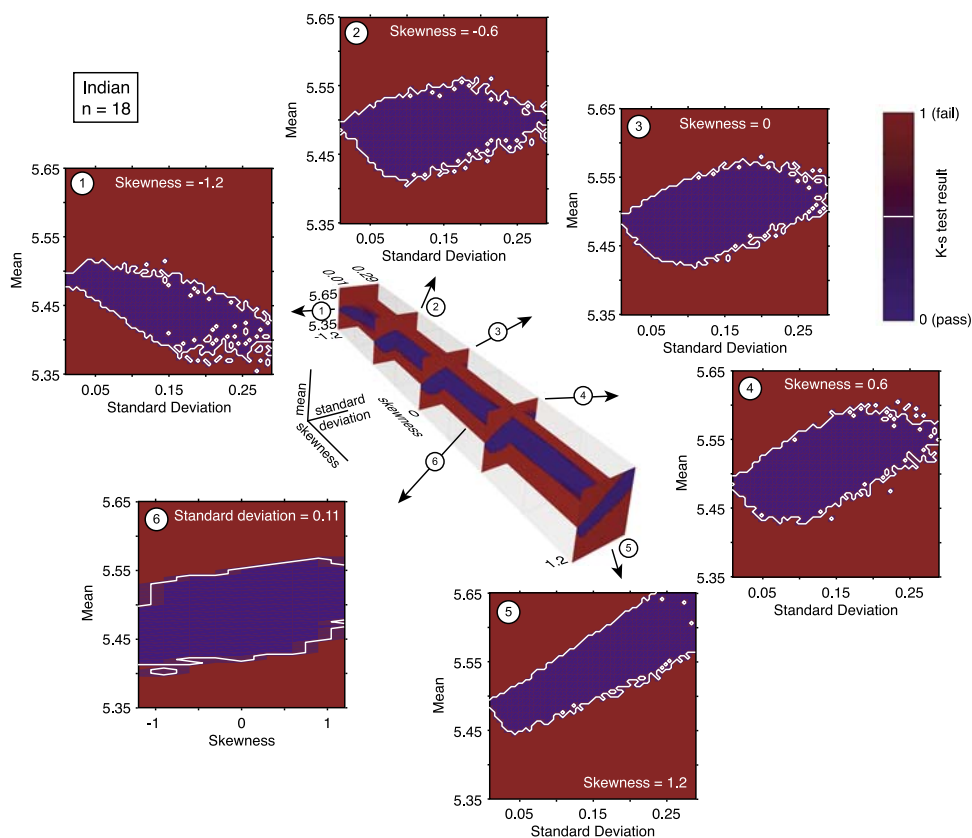
Figure 5b. Diagrams showing results of Monte Carlo simulations comparing different parent distributions with data for Atlantic MORB. See caption of Figure 5a for details, and see sections 4.2.2 and 4.2.3 for discussion.

furthermore the tradeoffs between mean and standard deviation become more important. Similar patterns hold for the Atlantic (Figure 5b) and Indian (Figure 5c) MORB data sets, although the range of acceptable parameters is slightly smaller for the Atlantic than for the Pacific, and considerably larger for the Indian than for either of the other two. For example, at skewness = 0, the total range of acceptable mean values is 0.07‰ (5.48–5.55) for the Atlantic and 0.1‰ (5.47–5.57‰) for the Pacific data, compared to 0.17‰ (5.41–5.58‰) for the Indian Ocean data (Table 3b). These simulations suggest that the mean and standard deviation of the MORB $\delta^{18}O$ data are a good estimate of the mean and standard deviation of the parent distribution, i.e., 5.52 ± 0.05‰ for the Pacific and Atlantic data, and 5.50 ± ~0.1‰ for the Indian data. On the other hand, the simulations show a wide range of skewness of the parent data set that would be consistent with the MORB data: each data set is consistent with skewness from −1.2 to 1.2 (with corresponding tradeoffs in allowable mean and standard deviation).

[30] A different approach to estimating confidence intervals of the mean, standard deviation, and skewness of the data is to compute confidence intervals through a bootstrap method. We computed 95% confidence intervals for each parameter in each MORB data set using sample sizes of 10,000, and results are presented in Table 3c. These confidence intervals are somewhat narrower than (but within the range of) the acceptable range of parameters yielded by the Monte Carlo approach. For example, the calculated 95% confidence interval on the mean is 5.49–5.55‰, 5.50–5.55‰, and 5.46–5.55 for Pacific, Atlantic, and Indian MORB data, respectively (Table 3c).

[31] One question that is not addressed by these simulations is why the Indian MORB data are consistent with significantly wider ranges of parameters for the parent distribution than are the Atlantic or Pacific MORB data. Is this due to the smaller sample size for Indian MORB data (n = 18, compared to n = 51 for Pacific and 62 for Atlantic) or to intrinsically more heterogeneity within the Indian MORB data? In order to test the possibility that small sample size limits the ability of this kind of simulation to constrain the parameters of the parent distribution, we performed a second set of Monte Carlo simulations where we compared sub-

Figure 5c. Diagrams showing results of Monte Carlo simulations comparing different parent distributions with data for Indian MORB. See caption of Figure 5a for details, and see sections 4.2.2 and 4.2.3 for discussion.

sets of synthetic data to the full 1000-sample synthetic data sets. In these simulations, we took random subsamples of different sizes (20, 50, or 100 data points) from the 1000-sample synthetic data set with mean 5.52, standard deviation 0.11 and skewness = 0, and compared that subsample to each 1000-sample synthetic data set for the full parameter range, effectively performing the same comparison as the Monte Carlo simulations with the real MORB data, but with a known parent distribution. The 1000-sample synthetic data sets were the same as those used in comparison with the MORB oxygen isotope data. Each simulation repeated the subsampling and comparison with the range of synthetic distributions 1000 times. This is a method of assessing how the Monte Carlo test

Table 3a. Summary of Statistical Parameters for MORB δ^{18}O Data

	n	Mean	Standard Deviation	Skewness
All MORB	131	5.52	0.10	0.18
Pacific	51	5.52	0.11	0.12
Atlantic	62	5.52	0.10	0.15
Indian	18	5.50	0.10	0.56

Table 3b. Summary of Results of Monte Carlo Simulations Comparing MORB Data to Potential Parent Distributions[a]

	Pacific	Atlantic	Indian
	Skewness = −1.2		
Mean	5.46−5.55	5.45−5.53	5.36−5.52
Standard deviation	0.05−0.18	0.03−0.14	0.01−0.29
	Skewness = −0.6		
Mean	5.46−5.56	5.48−5.54	5.40−5.57
Standard deviation	0.05−0.21	0.03−0.16	0.01−10.29
	Skewness = 0		
Mean	5.47−5.57	5.48−5.55	5.41−5.58
Standard deviation	0.05−0.21	0.03−0.18	0.01−0.29
	Skewness = 0.6		
Mean	5.49−5.58	5.49−5.57	5.48−5.59
Standard deviation	0.06−0.20	0.03−0.17	0.01−0.29
	Skewness = 1.2		
Mean	5.54−5.58	5.51−5.59	5.44−5.65
Standard deviation	0.12−0.18	0.03−0.17	0.01−0.29

[a] Shown are parameter combinations which are potential parent distributions of the MORB data.

Table 3c. Confidence Intervals for MORB Data Estimated by Bootstrap Method

	Mean	Standard Deviation	Skewness
All MORB	5.50−5.54	0.09−0.12	−0.19−0.57
Indian	5.46−5.55	0.08−0.13	−0.15−1.3
Pacific	5.49−5.55	0.09−0.13	−0.32−0.77
Atlantic	5.50−5.55	0.08−0.13	−0.53−0.89

procedure behaves when applied to a data set of similar size to the MORB data sets, but with known parent distribution parameters. Results for these simulations are shown in Figures 6a–6c, which plots the cumulative number of failed Kolmogorov-Smirnov tests after comparing each of the 1000 subsamples to the range of potential parent distributions. The plots are similar to those of the Kolmogorov-Smirnov tests of synthetic data to MORB data (Figures 5a–5c) but are color coded according to the number of failed Kolmogorov-Smirnov tests when comparing subsets of the synthetic test distribution to the other synthetic distributions. The white contour corresponds to a threshold where 95% of the subsets failed a Kolmogorov-Smirnov test with a synthetic distribution that has different statistical parameters than the test data. In other words, outside that contour, the test functions properly 95% of the time in terms of rejecting the null hypothesis that the two data sets are drawn from the same distribution. Within the contour, there are some "false positives" where the test fails to reject the null hypothesis even though it is false: there is only a single point on the diagrams (at mean = 5.52, standard deviation = 0.11, and skewness = 0) where the null hypothesis is, strictly speaking, true. Thus, in the region within the contour, the test is relatively insensitive to differences between the distributions tested. In the context of using the Monte Carlo simulations with the MORB data as hypothesis tests to determine which parameter combinations can be rejected, the contour where the Kolmogorov-Smirnov test correctly rejects the null hypothesis 95% of the time corresponds to the 95% confidence interval. Comparison of Figures 6a and 6b, where the subsets were of 50 samples and 20 samples, respectively, shows that the region where the null hypothesis cannot be rejected > 95% of the time is significantly larger for the simulation where smaller subsets were compared with the parent distributions. Thus, it is likely that the difference in range of acceptable parameters for the Indian MORB data compared to the Pacific or Atlantic MORB data in the first

Monte Carlo simulations is due simply to having a smaller data set.

[32] One interesting observation that falls out of this second set of Monte Carlo simulations is that in each case the region within the 95% contour becomes more elongate and less "equant" as the skewness of the test data set gets farther from the skewness of the parent distribution (in this case, zero). Although this does not place quantitative constraints on the skewness of the parent distributions for the MORB data, it suggests that the skewness of the parent distribution for the MORB data is close to zero (i.e., a normal distribution). Based on comparing results for the second set of Monte Carlo simulations with 20 versus 50 versus 100 data points in each subsample, it should be possible to further refine the limits on the statistical parameters of the parent distribution with additional laser fluorination measurements of MORB data. For example, it may be possible to more quantitatively identify a smaller acceptable range of skewness with sample sets of 100 or more (Figure 6c).

4.2.3. Implications for Upper Mantle Heterogeneity

[33] The similar range and mean value of the various MORB $\delta^{18}O$ subsets suggest that there is

Table 3d. Summary of Results of Monte Carlo Simulations Comparing Subsamples and Larger Samples of Parent Distributions[a]

	Subsample Size: $n = 20$	Subsample Size: $n = 50$	Subsample Size: $n = 100$
Skewness = −1.2			
Mean	5.35−5.61	5.43−5.58	5.49−5.53
Standard deviation	0.01−0.29	0.04−0.21	0.10−0.14
Skewness = −0.6			
Mean	5.39−5.62	5.44−5.58	5.46−5.56
Standard deviation	0.01−0.29	0.04−0.24	0.06−0.20
Skewness = 0			
Mean	5.41−5.64	5.45−5.60	5.47−5.57
Standard deviation	0.01−0.29	0.04−0.25	0.06−0.20
Skewness = 0.6			
Mean	5.43−5.65	5.46−5.60	5.48−5.58
Standard deviation	0.01−0.29	0.04−0.24	0.06−0.19
Skewness = 1.2			
Mean	5.45−5.65	5.47−5.61	5.52−5.55
Standard deviation	0.01−0.29	0.05−0.21	0.09−0.13

[a] Included are range of parameters where Kolmogorov-Smirnov test is insensitive to differences between the subsamples and the parent distributions.
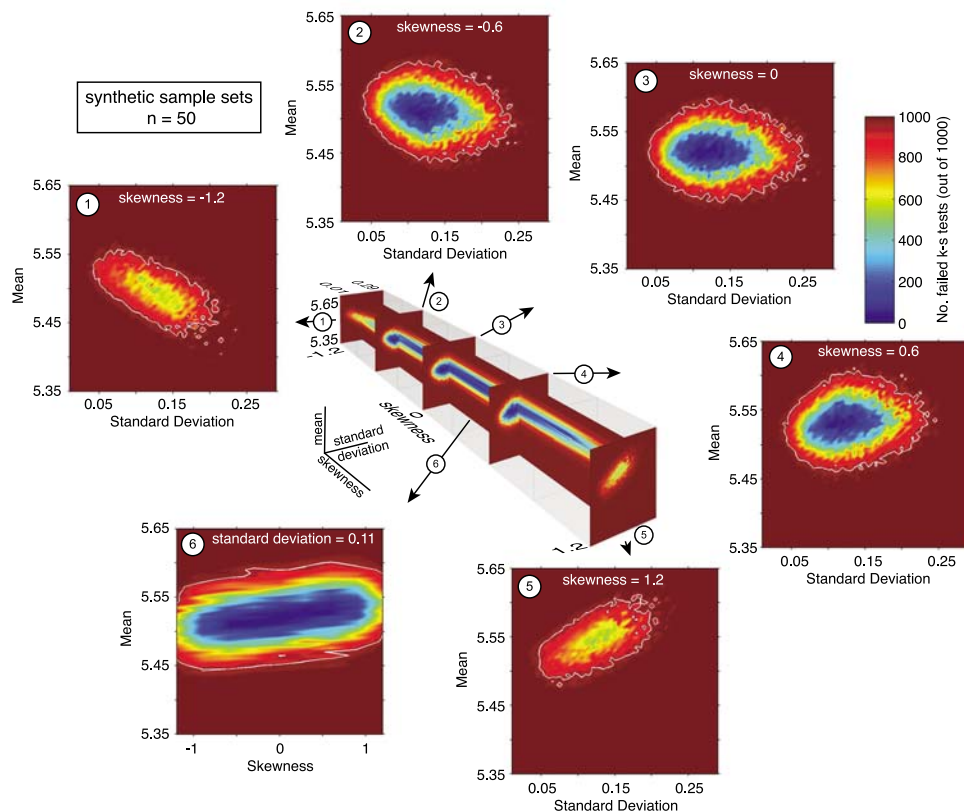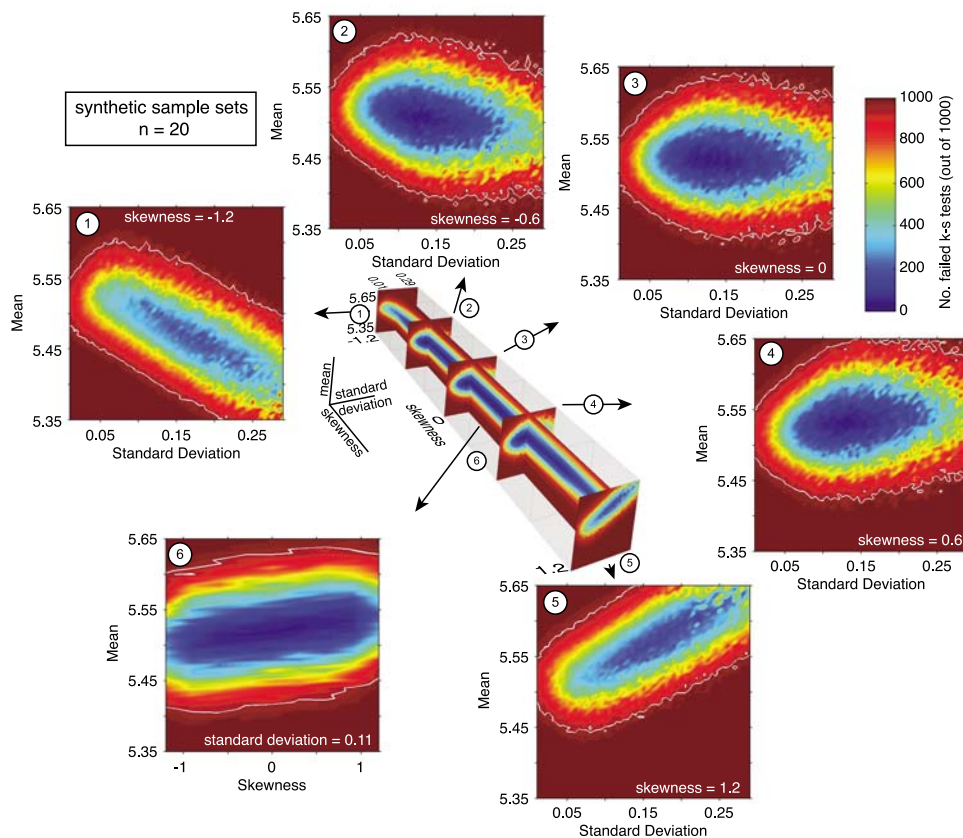
Figure 6a. Diagrams showing the results of Monte Carlo simulations comparing subsets of the synthetic sample data with a range of parent distributions. Synthetic data sets were taken as random subsamples of 50 samples of a parent distribution with mean of 5.52, standard deviation of 0.1, and skewness of 0. These synthetic data sets were compared to synthetic distributions (with a range of mean, standard deviation, and skewness) using a two-sample Kolmogorov-Smirnov test, and the process was repeated for 1000 different subsamples. The results are color coded by the cumulative number of failed Kolmogorov-Smirnov tests (indicating that the two data sets compared are not consistent with being derived from the same parent distribution), and the white contour represents a cumulative failure of 950 out of 1000 subsamples. Because the subsamples were all drawn from a single distribution in the center of the parameter space explored, the contour separates the region in which the Kolmogorov-Smirnov test correctly identifies distinctions between the parent distribution of the subsample data set and the parent distribution with other parameter combinations 95% of the time (outside of the contour) from the region where the Kolmogorov-Smirnov test is insensitive to differences in the statistical parameters of the parent data sets compared. See sections 4.2.2 and 4.2.3 for discussion.

a broadly reproducible process that controls the oxygen isotope composition of the upper mantle throughout the Earth and further suggests that the variability in $\delta^{18}O$ of MORB reflects the presence of a small but variable mass fraction of enriched material distributed within the upper mantle. The Monte Carlo simulations in turn suggest that (1) the means and standard deviations of MORB data for the different ocean basins are a robust measure of the mean and standard deviation of the "parent distribution" sampled (which physically is related to the percentage and spatial distribution of hetero-

geneities within the upper mantle and to the size of the region sampled during melting) and (2) the normal distributions of MORB sample data most likely reflect a normal parent distribution, although we cannot definitively rule out some skewness in the parent distribution. One implication is that melting of the upper mantle to produce MORB either samples the same fraction of enriched material (on average) and that $\delta^{18}O$ of that enriched material is relatively constant throughout the upper mantle globally, or that there is a fortuitous tradeoff between the average percentage of enriched mate-
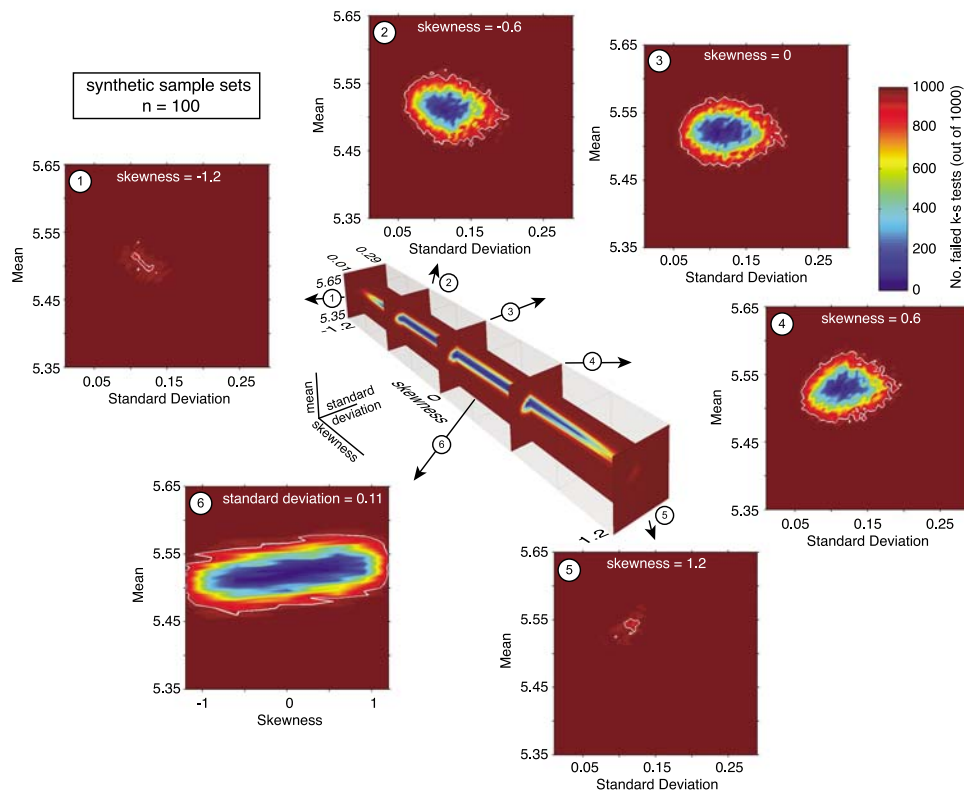
Figure 6b. Diagrams showing the results of Monte Carlo simulations comparing subsets of the synthetic sample data with a range of parent distributions. Synthetic data sets were taken as random subsamples of 20 samples of a parent distribution with mean of 5.52, standard deviation of 0.1, and skewness of 0. See caption of Figure 6a for further details, and see sections 4.2.2 and 4.2.3 for discussion.

rial sampled and the oxygen isotope composition of that enriched material such that the average $\delta^{18}O$ of MORB is the same across MORB globally. Furthermore, the narrow range of $\delta^{18}O$ in MORB ($\sim$0.5‰) relative to the crustal inputs during subduction (>40‰) implies either that the fraction of crustal material within the upper mantle is relatively small, or that the isotopically diverse constituents are very evenly mixed such that the region sampled during MORB melting always contains roughly the same mixture.

[34] It is possible that even the low-$\delta^{18}O$ end of the MORB spectrum reflects contributions from some component of crustal material; in particular, the lowermost altered oceanic crust on average has $\delta^{18}O$ lower than average for fresh MORB [e.g., *Alt and Teagle*, 2000], thus it is possible that incorporation of lower altered oceanic crust could have affected the low-$\delta^{18}O$ samples. However, in local-

ized studies where the crustal component can be identified [*Cooper et al.*, 2004; *Eiler et al.*, 2000b], the low-$\delta^{18}O$ end of the array corresponds to samples with other geochemical characteristics that commonly have been associated with the depleted end of the MORB array (e.g., low La/Sm, unradiogenic Pb and Sr and radiogenic Nd isotopes), instead of the relatively more enriched characteristics expected for low-$\delta^{18}O$ lower oceanic crust. Thus, the low-$\delta^{18}O$ end-member likely corresponds to relatively uncontaminated depleted upper mantle. Nevertheless, we cannot rule out the possibility that lower oceanic crust has contributed to the source of some of the low-$\delta^{18}O$ samples; as discussed by *Eiler et al.* [2000b, and references therein] the lower oceanic crust is relatively poor in trace elements, and the effects of hydrothermal alteration in oceanic crustal sections appear to decrease with depth in the gabbro section, such that the deepest gabbros sampled in situ show

Figure 6c. Diagrams showing the results of Monte Carlo simulations comparing subsets of the synthetic sample data with a range of parent distributions. Synthetic data sets were taken as random subsamples of 100 samples of a parent distribution with mean of 5.52, standard deviation of 0.1, and skewness of 0. See caption of Figure 6a for further details, and see sections 4.2.2 and 4.2.3 for discussion.

relatively little contrast in $\delta^{18}O$ compared to fresh MORB [*Alt and Teagle*, 2000]. Therefore, the global MORB data may include samples which reflect a relatively subtle influence of recycled lower oceanic crust, and this may contribute to the scatter in the data arrays.

[35] If the low-$\delta^{18}O$ end of the MORB spectrum (~5.25‰) is assumed to represent ambient, depleted upper mantle free of the influence of crust, than the range of ~0.5‰ in MORB glasses implies the presence of up to ~10% crustal material with average $\delta^{18}O$ of 10‰ (similar to estimates of average values for altered volcanic rocks of the upper oceanic crust and, as discussed above, to the average of Australian lower crustal xenoliths [e.g., *Alt and Teagle*, 2000; *Harmon and Hoefs*, 1995; *Kempton and Harmon*, 1992; *Staudigel et al.*, 1996]). The average value of $\delta^{18}O$ in the MORB data sets (~5.52‰) would then correspond to an average of ~5% crustal material within the upper mantle. If the crustal material included a large

fraction of sediment, the implied mass fraction of crustal material would be as much as 5 times smaller; i.e., varying from 0 to 10% and averaging ~1%; however, such a large fraction of sediment would affect the Sr isotope systematics of the data to a much larger extent, producing higher $^{87}Sr/^{86}Sr$ at a given $\delta^{18}O$ than is observed (e.g., compare Figure 4 to *Cooper et al.* [2004] and *Eiler et al.* [2000b]). Although we cannot rule out the influence of a small percentage of sediment within the upper mantle (as was discussed above for the AAD samples), the constant mean $\delta^{18}O$ between ocean basins does imply that there cannot be a significant difference between the amount of sediment present in the upper mantle of the different ocean basins. Given that the combined oxygen isotope, radiogenic isotope, and trace element characteristics of subsets of the MORB data are consistent with the presence of crustal material with broadly similar average $\delta^{18}O$ of ~10‰ (lower crust in the case of AAD Indian samples, altered oceanic crust in the case of NMORB and Mid-Atlantic Ridge data [*Cooper et al.*, 2004;

Eiler et al., 2000b]), we suggest that the influence of sediment on the oxygen isotope composition of the upper mantle in general is limited.

[36] Our estimates of the amount of crustal material distributed within the upper mantle are broadly consistent with other estimates. For example, *Hofmann* [1997] calculated that subduction of oceanic lithosphere injects ~20 km^3/yr of crustal and sedimentary material into the mantle and that over 4.55 Gyr this would inject crust equivalent to a total of 7.5% of the mass of the mantle. In a similar calculation, *Stracke et al.* [1999] calculated that recycled crust should account for 8–10% of the mantle. Our estimate of an average of ~5% crustal material in the MORB source is also consistent with the recent quantitative estimate of ~4% recycled crustal material in the MORB source, based on major element and compatible trace element analyses of olivine [*Sobolev et al.*, 2007].

[37] One implication of the similarity in mean and standard deviation of $\delta^{18}O$ between ocean basins is that the differences in radiogenic isotope composition between MORB of the Indian and Pacific or Atlantic basins may reflect the age and specific nature of enriched material within the upper mantle rather than variations in its abundance. For example, *Eiler et al.* [2000b] concluded based on correlations between trace element ratios and $\delta^{18}O$ in NMORB that the upper mantle MORB source contains an average of 2% enriched material derived from upper oceanic crust (in the proportions 95% altered basaltic crust and 5% sediment). Similarly, *Cooper et al.* [2004] also concluded that the variations in $\delta^{18}O$ in samples of the Mid-Atlantic Ridge resulted from the incorporation of an average of 2–5% material derived from altered oceanic crust. However, in this case the relations between trace elements, radiogenic isotopes, and $\delta^{18}O$ require a different mechanism where partial melts of upper altered oceanic basaltic crust (with very little addition of sediment) metasomatized the upper mantle at approximately 250 Ma [also see *Donnelly et al.*, 2004]. Although back-arc basin basalts (BABB) were not included in this study, some of them share similar $\delta^{18}O$ trace element characteristics to MORB and may reflect similar processes [e.g., *Bonifacie et al.*, 2008; *Macpherson et al.*, 2000]. Other detailed studies of $\delta^{18}O$ combined with trace element and radiogenic isotope measurements in MORB from specific geographic areas or with restricted geochemical characteristics could test this hypothesis, as well as extending the data set that could be used to further refine the characteristics of the parent distribution.

5. Conclusions

[38] Pacific-type and Indian-type MORB at the AAD show no systematic differences in oxygen isotope composition. This observation is inconsistent with an origin of Indian-type mantle by the addition of pelagic sediment not present in the Pacific upper mantle. However, combined radiogenic isotope, trace element and oxygen isotope characteristics of I-type MORB at the AAD are consistent with an origin by contamination of the Indian upper mantle by lower crustal material [e.g., *Escrig et al.*, 2004; *Hanan et al.*, 2004].

[39] This similarity in characteristics of the $\delta^{18}O$ data between ocean basins holds in the global database of laser fluorination $\delta^{18}O$ data for MORB. The similarity in mean and standard deviation of data for the Indian, Pacific, and Atlantic ocean basins, together with correlations of $\delta^{18}O$ with radiogenic isotope and trace element characteristics of subsets of the data, suggest that the upper mantle globally contains an average of ~5–10% recycled crustal material, and that the depleted mantle has $\delta^{18}O$ of ~5.25–5.30‰. Furthermore, the data rule out significant differences in the percentage of sediment in the upper mantle in any one ocean basin compared to the other two.

[40] The normal distribution of the global MORB $\delta^{18}O$ data set suggests that a stochastic process is producing the observed variations; the Monte Carlo simulations we performed suggest that the "parent distribution" is most likely normal as well (although some skewness in the parent distribution cannot be ruled out), and that the variance in the data is larger than is consistent with random analytical error; therefore, some geologic process must have produced the variations. These inferences are most consistent with a well-stirred upper mantle, that is, where the physical distribution of heterogeneities is random. Further, the variance of the distribution, which is small compared to the inferred range in $\delta^{18}O$ of ambient depleted mantle versus enriched crustal material, suggests that the size of the sampling region is large compared to the size of enriched domains. Finally, the mean of the sample data sets appears to be a robust indicator of the mean of $\delta^{18}O$ in the upper mantle sampled, which in turn implies a small but consistent percentage of enriched crust distributed within the upper mantle globally.

[41] Although a full treatment of the problem is beyond the scope of this manuscript, the Monte Carlo simulations also suggest that the patterns of data presented here provide constraints on the physical distribution of crustal material within the upper mantle and the distribution of data produced upon sampling through melting. Therefore, these data could in the future provide a test of geodynamic models of crustal recycling and mixing by comparing the distribution of MORB $\delta^{18}O$ data to a systematic exploration of the distribution of data expected from different geodynamic models.

Acknowledgments

References

Albarede, F. (2001), Radiogenic ingrowth in systems with multiple reservoirs: Applications to the differentiation of the mantle-crust system, *Earth Planet. Sci. Lett.*, *189*, 59–73, doi:10.1016/S0012-821X(01)00350-8.

Allegre, C. J., B. Hamelin, and B. Dupre (1984), Statistical analysis of isotopic ratios in MORB: The mantle blob cluster model and the convective regime of the mantle, *Earth Planet. Sci. Lett.*, *71*, 71–84, doi:10.1016/0012-821X(84)90053-0.

Allegre, C. J., B. Hamelin, A. Provost, and B. Dupre (1987), Topology in isotopic multispace and origin of mantle chemical heterogeneities, *Earth Planet. Sci. Lett.*, *81*, 319–337, doi:10.1016/0012-821X(87)90120-8.

Alt, J. C., and D. A. H. Teagle (2000), Hydrothermal alteration and fluid fluxes in ophiolites and oceanic crust, in *Ophiolites and Ocean Crust: New Insights From Field Studies and Ocean Drilling Program*, edited by Y. Dilek et al., *Spec. Pap. Geol. Soc. Am.*, *349*, 273–282.

Billen, M. I., O. Kereylos, B. Hamman, M. Jadamec, L. H. Kellogg, O. Staadt, and D. Y. Sumner (2008), A geoscience perspective on immersive 3D data visualization, *Comput. Geosci.*, *34*, 1056–1072, doi:10.1016/j.cageo.2007.11.009.

Bonifacie, M., J. M. Eiler, E. M. Stolper, A. Bezos, P. Michael, and C. H. Langmuir (2008), Oxygen isotope evidence for slab-derived silicate melt in Lau basin back-arc lavas, *Geochim. Cosmochim. Acta*, *72*, A96.

Brandenburg, J. P., E. H. Hauri, P. E. van Keken, and C. J. Ballentine (2008), A multiple-system study of the geochemical evolution of the mantle with force-balanced plates and thermochemical effects, *Earth Planet. Sci. Lett.*, *276*, 1–13, doi:10.1016/j.epsl.2008.08.027.

Christensen, U. R., and A. W. Hofmann (1994), Segregation of subducted oceanic crust in the convecting mantle, *J. Geophys. Res.*, *99*, 19,867–19,884, doi:10.1029/93JB03403.

Christie, D. M., B. P. West, D. G. Pyle, and B. B. Hanan (1998), Chaotic topography, mantle flow and mantle migration in the Australian-Antarctic discordance, *Nature*, *394*, 637–644, doi:10.1038/29226.

Christie, D. M., D. G. Pyle, R. B. Pedersen, and D. J. Miller (2004), Leg 187 synthesis: Evolution of the Australian Antarctic Discordance, the Australian Antarctic depth anomaly, and the Indian/Pacific mantle isotopic boundary, *Proc. Ocean Drill. Program Sci. Results*, *187*, 1–41.

Cohen, R. S., N. M. Evensen, P. J. Hamilton, and R. K. O'Nions (1980), U-Pb, Sm-Nd and Rb-Sr systematics of mid-ocean ridge basalt glasses, *Nature*, *283*, 149–153, doi:10.1038/283149a0.

Cooper, K. M., J. M. Eiler, P. D. Asimow, and C. H. Langmuir (2004), Oxygen-isotope evidence for the origin of enriched mantle beneath the mid-Atlantic ridge, *Earth Planet. Sci. Lett.*, *220*, 297–316, doi:10.1016/S0012-821X(04)00058-5.

Donnelly, K. E., S. L. Goldstein, C. H. Langmuir, and M. Spiegelman (2004), Origin of enriched ocean ridge basalts and implications for mantle dynamics, *Earth Planet. Sci. Lett.*, *226*, 347–366, doi:10.1016/j.epsl.2004.07.019.

Dupre, B., and C. J. Allegre (1983), Pb-Sr isotope variation in Indian Ocean basalts and mixing phenomena, *Nature*, *303*, 142–146, doi:10.1038/303142a0.

Eiler, J. M. (2001), Oxygen isotope variations of basaltic lavas and upper mantle rocks, *Rev. Mineral. Geochem.*, *43*, 319–364, doi:10.2138/gsrmg.43.1.319.

Eiler, J. M., K. A. Farley, J. W. Valley, E. Hauri, H. Craig, S. R. Hart, and E. M. Stolper (1997), Oxygen isotope variations in ocean island basalt phenocrysts, *Geochim. Cosmochim. Acta*, *61*, 2281–2293, doi:10.1016/S0016-7037(97)00075-6.

Eiler, J. M., A. Crawford, T. Elliott, K. A. Farley, J. W. Valley, and E. M. Stolper (2000a), Oxygen isotope geochemistry of oceanic-arc lavas, *J. Petrol.*, *41*, 229–256, doi:10.1093/petrology/41.2.229.

Eiler, J. M., P. Schiano, N. Kitchen, and E. M. Stolper (2000b), Oxygen-isotope evidence for recycled crust in the sources of mid-ocean-ridge basalts, *Nature*, *403*, 530–534, doi:10.1038/35000553.

Eiler, J. M., M. J. Carr, M. Reagan, and E. Stolper (2005), Oxygen isotope constraints on the sources of Central American arc lavas, *Geochem. Geophys. Geosyst.*, *6*, Q07007, doi:10.1029/2004GC000804.

Elkins, L. J., G. A. Gaetani, and K. W. W. Sims (2008), Partitioning of U and Th during garnet pyroxenite partial melting: Constraints on the source of alkaline ocean island basalts, *Earth Planet. Sci. Lett.*, *265*, 270–286, doi:10.1016/j.epsl.2007.10.034.

Escrig, S., F. Capmas, B. Dupre, and C. J. Allegre (2004), Osmium isotopic constraints on the nature of the DUPAL anomaly from Indian mid-ocean-ridge basalts, *Nature*, *431*, 59–63, doi:10.1038/nature02904.

Goldstein, S. L., G. Soffer, C. H. Langmuir, K. A. Lehnert, D. W. Graham, and P. J. Michael (2008), Origin of a 'Southern Hemisphere' geochemical signature in the Arctic upper mantle, *Nature*, *453*, 89–94, doi:10.1038/nature06919.

Gurnis, M., and R. D. Muller (2003), Origin of the Australian-Antarctic Discordance from an ancient slab and mantle wedge, in *Evolution and Dynamics of the Australian Plate*, edited by R. R. Hills and R. D. Muller, *Spec. Pap. Geol. Soc. Am.*, *372*, 417–429.

Gurnis, M., R. D. Muller, and L. Moresi (1998), Cretaceous vertical motion of Australia and the Australian-Antarctic Discordance, *Science*, *279*, 1499–1504, doi:10.1126/science.279.5356.1499.

Hanan, B. B., J. Blichert-Toft, D. G. Pyle, and D. M. Christie (2004), Contrasting origins of the upper mantle revealed by hafnium and lead isotopes from the Southeast Indian Ridge, *Nature*, *432*, 91–94, doi:10.1038/nature03026. (Corrigendum, *432*, 653, doi:10.1038/nature03181, 2004.)

Harmon, R. S., and J. Hoefs (1995), Oxygen isotope heterogeneity of the mantle deduced from global ^{18}O systematics of basalts from different geotectonic settings, *Contrib. Mineral. Petrol.*, *120*, 95–114, doi:10.1007/BF00311010.

Hart, S. R. (1971), K, Rb, Cs, Sr, Ba contents and Sr isotope ratios of ocean floor basalts, *Philos. Trans. R. Soc. London, Ser. A*, *268*, 573–587.

Hart, S. R. (1984), A large-scale isotope anomaly in the Southern Hemisphere mantle, *Nature*, *309*, 753–757, doi:10.1038/309753a0.

Hawkesworth, C. J., M. S. M. Mantovani, P. N. Taylor, and Z. Palacz (1986), Evidence from the Parana of south Brazil for a continental contribution to Dupal basalts, *Nature*, *322*, 356–359, doi:10.1038/322356a0.

Hirschmann, M. M., and E. M. Stolper (1996), A possible role for garnet pyroxenite in the origin of the "garnet signature" in MORB, *Contrib. Mineral. Petrol.*, *124*, 185–208, doi:10.1007/s004100050184.

Hofmann, A. W. (1997), Mantle geochemistry: The message from oceanic volcanism, *Nature*, *385*, 219–229, doi:10.1038/385219a0.

Hofmann, A. W. (2003), Sampling mantle heterogeneity through oceanic basalts: Isotopes and trace elements, in *The Mantle and Core*, edited by R. W. Carlson, pp. 61–101, Elsevier, New York.

Ito, E., W. M. White, and C. Gopel (1987), The O, Sr, Nd and Pb isotope geochemistry of MORB, *Chem. Geol.*, *62*, 157–176, doi:10.1016/0009-2541(87)90083-0.

Janney, P. E., A. P. le Roex, and R. W. Carlson (2005), Hafnium isotope and trace element constraints on the nature of mantle heterogeneity beneath the central Southwest Indian Ridge, *J. Petrol.*, *46*, 2427–2464, doi:10.1093/petrology/egi060.

Kellogg, L. H., B. H. Hager, and R. D. van der Hilst (1999), Compositional stratification in the deep mantle, *Science*, *283*, 1881–1884, doi:10.1126/science.283.5409.1881.

Kellogg, J. B., S. B. Jacobsen, and R. J. O'Connell (2002), Modeling the distribution of isotopic ratios in geochemical reservoirs, *Earth Planet. Sci. Lett.*, *204*, 183–202, doi:10.1016/S0012-821X(02)00981-0.

Kellogg, J. B., S. B. Jacobsen, and R. J. O'Connell (2007), Modeling lead isotope heterogeneity in mid-ocean ridge basalts, *Earth Planet. Sci. Lett.*, *262*, 328–342, doi:10.1016/j.epsl.2007.06.018.

Kempton, P. D., and R. S. Harmon (1992), Oxygen isotope evidence for large-scale hybridization of the lower crust during magmatic underplating, *Geochim. Cosmochim. Acta*, *56*, 971–986, doi:10.1016/0016-7037(92)90041-G.

Kempton, P. D., J. A. Pearce, T. L. Barry, J. G. Fitton, C. Langmuir, and D. M. Christie (2002), Sr-Nd-Pb-Hf isotope results from ODP Leg 187: Evidence for mantle dynamics of the Australian-Antarctic Discordance and origin of the Indian MORB source, *Geochem. Geophys. Geosyst.*, *3*(12), 1074, doi:10.1029/2002GC000320.

Klein, E. M., C. H. Langmuir, A. Zindler, H. Staudigel, and B. Hamelin (1988), Isotope evidence of a mantle convection boundary at the Australian-Antarctic Discordance, *Nature*, *333*, 623–629, doi:10.1038/333623a0.

Klein, E. M., C. H. Langmuir, and H. Staudigel (1991), Geochemistry of basalts from the Southeast Indian Ridge, 115°E–138°E, *J. Geophys. Res.*, *96*, 2089–2107, doi:10.1029/90JB01384.

Kogiso, T., M. M. Hirschmann, and D. J. Frost (2003), High-pressure partial melting of garnet pyroxenite: Possible mafic lithologies in the source of ocean island basalts, *Earth Planet. Sci. Lett.*, *216*, 603–617, doi:10.1016/S0012-821X(03)00538-7.

Kogiso, T., M. M. Hirschmann, and P. W. Reiners (2004), Length scales of mantle heterogeneities and their relationship to ocean island basalt chemistry, *Geochim. Cosmochim. Acta*, *68*, 345–360, doi:10.1016/S0016-7037(03)00419-8.

Macpherson, C. G., J. A. Gamble, and D. P. Mattey (1998), Oxygen isotope geochemistry of lavas from an oceanic to continental arc transition, Kermadec-Hikurangi margin, SW Pacific, *Earth Planet. Sci. Lett.*, *160*, 609–621, doi:10.1016/S0012-821X(98)00115-0.

Macpherson, C. G., D. R. Hilton, D. P. Mattey, and J. M. Sinton (2000), Evidence for an ^{18}O-depleted mantle plume from contrasting ^{18}O/^{16}O ratios of back-arc lavas from the Manus Basin and Mariana Trough, *Earth Planet. Sci. Lett.*, *176*, 171–183, doi:10.1016/S0012-821X(00)00002-9.

Mahoney, J., C. Nicollet, and C. Dupuy (1991), Madagascar basalts: Tracking oceanic and continental sources, *Earth Planet. Sci. Lett.*, *104*, 350–363, doi:10.1016/0012-821X(91)90215-4.

Mattey, D., D. Lowry, and C. Macpherson (1994), Oxygen isotope composition of mantle peridotite, *Earth Planet. Sci. Lett.*, *128*, 231–241, doi:10.1016/0012-821X(94)90147-3.

Meibom, A., and D. L. Anderson (2004), The statistical upper mantle assemblage, *Earth Planet. Sci. Lett.*, *217*, 123–139, doi:10.1016/S0012-821X(03)00573-9.

Pertermann, M., and M. M. Hirschmann (2003), Anhydrous partial melting experiments on MORB-like eclogite: Phase relations, phase compositions and mineral-melt partitioning of major elements at 2–3 GPa, *J. Petrol.*, *44*, 2173–2201, doi:10.1093/petrology/egg074.

Prinzhofer, A., E. Lewin, and C. J. Allegre (1989), Stochastic melting of the marble cake mantle: Evidence from local study of the East Pacific Rise at 12°50′N, *Earth Planet. Sci. Lett.*, *92*, 189–206, doi:10.1016/0012-821X(89)90046-0.

Pyle, D. G., D. M. Christie, and J. J. Mahoney (1992), Resolving an isotopic boundary within the Australian-Antarctic Discordance, *Earth Planet. Sci. Lett.*, *112*, 161–178, doi:10.1016/0012-821X(92)90014-M.

Pyle, D. G., D. M. Christie, J. J. Mahoney, and R. A. Duncan (1995), Geochemistry and geochronology of ancient southeast Indian and southwest Pacific seafloor, *J. Geophys. Res.*, *100*, 22,261–22,282, doi:10.1029/95JB01424.

Rehkämper, M., and A. W. Hofmann (1997), Recycled ocean crust and sediment in Indian Ocean MORB, *Earth Planet. Sci. Lett.*, *147*, 93–106, doi:10.1016/S0012-821X(97)00009-5.

Reiners, P. W. (2002), Temporal-compositional trends in intraplate basalt eruptions: Implications for mantle heterogeneity and melting processes, *Geochem. Geophys. Geosyst.*, *3*(02), 1011, doi:10.1029/2001GC000250.

Rudge, J. F., D. Mckenzie, and P. Haynes (2005), A theoretical approach to understanding the isotopic heterogeneity of mid-ocean ridge basalt, *Geochim. Cosmochim. Acta*, *69*, 3873–3887, doi:10.1016/j.gca.2005.03.004.

Rudnick, R. L. (1990), Nd and Sr isotopic compositions of lower-crustal xenoliths from north Queensland, Australia: Implications for Nd model ages and crustal growth processes, *Chem. Geol.*, *83*, 195–208, doi:10.1016/0009-2541(90)90280-K.

Rudnick, R. L., and S. J. Goldstein (1990), The Pb isotopic compositions of lower crustal xenoliths and the evolution of lower crustal Pb, *Earth Planet. Sci. Lett.*, *98*, 192–207, doi:10.1016/0012-821X(90)90059-7.

Salters, V. J. M., and A. Stracke (2004), Composition of the depleted mantle, *Geochem. Geophys. Geosyst.*, *5*, Q05B07, doi:10.1029/2003GC000597.

Schiano, P., J.-L. Birck, and C. J. Allegre (1997), Osmium-strontium-neodymium-lead isotopic covariations in mid-ocean ridge basalt glasses and the heterogeneity of the upper mantle, *Earth Planet. Sci. Lett.*, *150*, 363–379, doi:10.1016/S0012-821X(97)00098-8.

Schilling, J.-G., M. Zajac, R. Evans, T. Johnston, W. White, J. D. Devine, and R. Kingsley (1983), Petrologic and geochemical variations along the Mid-Atlantic Ridge from 29°N to 73°N, *Am. J. Sci.*, *283*, 510–586.

Sharp, Z. D. (1990), A laser-based microanalytical method for the in situ determination of oxygen isotope ratios of silicates and oxides, *Geochim. Cosmochim. Acta*, *54*, 1353–1357, doi:10.1016/0016-7037(90)90160-M.

Sims, K. W. W., et al. (2002), Chemical and isotopic constraints on the generation and transport of melt beneath the East Pacific Rise, *Geochim. Cosmochim. Acta*, *66*, 3481–3504, doi:10.1016/S0016-7037(02)00909-2.

Sims, K. W. W., et al. (2003), Aberrant youth: Chemical and isotopic constraints on the origin of off-axis lavas from the East Pacific Rise, 9°–10°N, *Geochem. Geophys. Geosyst.*, *4*(10), 8621, doi:10.1029/2002GC000443.

Sobolev, A. V., et al. (2007), The amount of recycled crust in sources of mantle-derived melts, *Science*, *316*, 412–417, doi:10.1126/science. 1138113.

Staudigel, H., T. Plank, W. M. White, and H. Schminke (1996), Geochemical fluxes during seafloor alteration of the upper oceanic crust: DSDP Sites 417 and 418, in *Subduction From Top to Bottom*, *Geophys. Monogr. Ser.*, vol. 96, edited by G. Bebout and S. Kirby, pp. 19–38, AGU, Washington, D. C.

Stracke, A., V. J. M. Salters, and K. W. W. Sims (1999), Assessing the presence of garnet-pyroxenite in the mantle sources of basalts through combined hafnium-neodymium-thorium isotope systematics, *Geochem. Geophys. Geosyst.*, *1*(12), 1006, doi:10.1029/1999GC000013.

Tackley, P. J. (2000), Mantle convection and plate tectonics: Toward an integrated physical and chemical theory, *Science*, *288*, 2002–2007, doi:10.1126/science.288.5473.2002.

Tatsumoto, M., C. Hedge, and A. E. J. Engel (1965), Potassium, rubidium, strontium, thorium, uranium, and the ratio of strontium-87 to strontium-86 in oceanic tholeiitic basalt, *Science*, *150*, 886–888, doi:10.1126/science.150.3698.886.

Valley, J. W., N. Kitchen, M. J. Kohn, C. R. Niendorff, and M. J. Spicuzza (1995), Strategies for high precision oxygen isotope analysis by laser fluorination, *Geochim. Cosmochim. Acta*, *59*, 5223–5231, doi:10.1016/0016-7037(95)00386-X.

van Keken, P. E., E. H. Hauri, and C. J. Ballentine (2002), Mantle mixing: The generation, preservation, and destruction of chemical heterogeneity, *Annu. Rev. Earth Planet. Sci.*, *30*, 493–525, doi:10.1146/annurev.earth.30.091201.141236.

Vervoort, J. D., P. J. Patchett, F. Albarede, J. Blichert-Toft, R. Rudnick, and H. Downes (2000), Hf-Nd isotopic evolution of the lower crust, *Earth Planet. Sci. Lett.*, *181*, 115–129, doi:10.1016/S0012-821X(00)00170-9.

White, W. M., and A. W. Hofmann (1982), Sr and Nd isotope geochemistry of oceanic basalts and mantle evolution, *Nature*, *296*, 821–825, doi:10.1038/296821a0.

Workman, R. K., and S. R. Hart (2005), Major and trace element composition of the depleted MORB mantle (DMM), *Earth Planet. Sci. Lett.*, *231*, 53–72, doi:10.1016/j.epsl. 2004.12.005.

Workman, R. K., J. M. Eiler, S. R. Hart, and M. G. Jackson (2008), Oxygen isotopes in Samoan lavas: Confirmation of continent recycling, *Geology*, *36*, 551–554, doi:10.1130/G24558A.1.

Xie, S., and P. J. Tackley (2004), Evolution of U-Pb and Sm-Nd systems in numerical models of mantle convection and plate tectonics, *J. Geophys. Res.*, *109*, B11204, doi:10.1029/2004JB003176.

Zindler, A., and S. Hart (1986), Chemical geodynamics, *Annu. Rev. Earth Planet. Sci.*, *14*, 493–571, doi:10.1146/annurev.ea.14.050186.002425.